



An efficient modelling approach for probabilistic assessments of present-day and future fluvial flooding.

Hieu Ngo^{1,2}, Roshanka Ranasinghe^{1,3,4}, Chris Zevenbergen^{1,2}, Ebru Kirezci⁵, Dikman Maheng^{1,2,6}, Mohanasundar Radhakrishnan⁷, Assela Pathirana^{1,8,9}

¹Department of Coastal and Urban Risk and Risk Resilience, IHE Delft Institute for Water Education, Delft, 2601 DA, The Netherlands

²Department of Hydraulic Engineering, Faculty of Civil Engineering and Geosciences, Delft University of Technology, Delft, 2628 CN, The Netherlands

³Department of Water Engineering and Management, University of Twente, Enschede, 7500 AE, The Netherlands

⁴Harbour, Coastal and Offshore engineering, Deltares, Delft, 2600 MH, The Netherlands

⁵Department of Infrastructure Engineering, University of Melbourne, Melbourne, Australia

⁶Department of Environmental Engineering, Universitas Muhammadiyah Kendari, Jl. Ahmad Dahlan 10, 93117, Kendari, Indonesia

⁷Agile Lotus Advisory, 104 Singel, 3112GS, Schiedam, The Netherlands

⁸United Nations Development Programme, 4th Floor, H. Aaage (Bank of Ceylon Building), Boduthakurufaanu Magu, Malé, The Maldives

⁹Ministry of environment, the government of the Maldives, Green Building, Malé, The Maldives

Correspondence to: Assela Pathirana (assela@pathirana.net)

Abstract. Flood risk management and planning decisions in many parts of the world have historically utilised flood hazard or risk maps for a very limited number of hazard scenarios (e.g. river water levels), mainly due to computational challenges. With the potentially massive increase in flood risk in future due to the combination of climate change effects (increasing the hazard) and increasing population and developments in floodplains (increasing the consequence), risk-informed flood risk management, which enables balancing the risk with the reward, is now becoming more and more sought after. This requires a comprehensive and quantitative risk assessment, which in turn demands multiple (thousands of) river and flood model simulations. Performing such a large number of model simulations is a challenge, especially for large, complex river systems (e.g. Mekong) due to the associated computational and resource demands. This article presents an efficient probabilistic modelling approach that combines a simplified 1D hydrodynamic model for the entire Mekong Delta with a detailed 1D/2D coupled model and demonstrates its application at Can Tho city in the Mekong Delta. Probabilistic flood hazard maps, ranging from 0.5 yr to 100 yr return period events, are obtained for the urban centre of Can Tho city under different future scenarios taking into account the impact of climate change forcing (river flow, sea-level rise, storm surge) and land subsidence. Results obtained under present conditions show that more than 12 % of the study area is inundated by the present-day 100 yr return period of water level. Future projections show that, if the present rate of land subsistence continues, by 2050 (under both RCP 4.5 and RCP 8.5 climate scenarios), the 0.5 yr and 100 yr return period flood extents will increase by around 15-fold and 8-fold, respectively, relative to the present-day flood extent. However, without land subsidence, the projected increases in the 0.5 yr and 100 yr return period flood extents by 2050 (under RCP 4.5 and RCP 8.5) are limited to between a



doubling to tripling of the present-day flood extent. Therefore, adaptation measures that can reduce the rate of land subsidence (e.g. limiting groundwater extraction), would substantially mitigate future flood hazards in the study area. A combination of restricted groundwater extraction and the construction of a new and more efficient urban drainage network would facilitate even further reductions in the flood hazard. The projected 15-fold increase in flood extent projected by 2050 for the twice per
40 year (0.5 yr return period) flood event implies that the “do nothing” management approach is not a feasible option for Can Tho.

1 Introduction

Flooding is one of the most frequently occurring and damaging natural disasters in the world (Hirabayashi et al., 2013; Kundzewicz et al., 2014; Arnell and Gosling, 2016; Alfieri et al., 2017; Forzieri et al., 2017; Mora et al., 2018). Coastal and
45 delta areas are among the most flood hazard-prone areas of the world (Nicholls, 2004; Nicholls et al., 2007; Wong et al., 2014; Neumann et al., 2015; Pasquier et al., 2018), and flood intensity and frequency are already increasing, especially in coastal and delta cities, due to changes in river flows, downstream sea-level and local changes in rainfall and land use (Merz et al., 2010; Balica et al., 2012; Huong and Pathirana, 2013; Chen et al., 2018). Coastal and delta regions are also among the most densely populated areas of the world, which have experienced a rapid expansion of settlements, urbanisation, infrastructure,
50 economic activities, and tourism especially over the last 5 decades or so (Small and Nicholls, 2003; Valiela et al., 2006; Ranasinghe and Jongejan, 2018).

Flood risk assessment is performed to facilitate the implementation of risk-informed measures aimed at minimizing (or mitigating) flood damage (Hall et al., 2003; Meyer et al., 2009, Bureau Reclamation, 2020; Mishra and Sinha, 2020). Flood hazard estimation, which computes the probability and intensity of a possible event (Pappenberger et al., 2012; Alfieri et al.,
55 2013; De Moel et al., 2015) is the first step in flood risk assessment (Penning-Rowsell et al., 2005; De Moel et al., 2015; Foudi et al., 2015; Kvočka et al., 2016). However, flood risk management and planning decisions in many parts of the world have historically utilised flood hazard or risk maps associated with one or two pre-determined return period water levels. While this may have been sufficient in the past, the need to move from stationary to innovative time-dependent (non-stationary) flood hazard and risk modelling approaches that can account for the uncertainty, arising from anthropogenic and climatic induced
60 stressors, is rapidly increasing (Mosavi et al., 2018).

Climate change is now recognized as a major global challenge in the 21st century and beyond. Future projections indicate that climate change will have implications on the trends of extreme events (e.g. extreme precipitation, hurricanes, etc.), which may lead to increases of flooding in the future (Panagoulia and Dimou, 1997; Menzel et al., 2002; Prudhomme et al., 2013; Alfieri et al., 2015). Besides the challenges posed by climate change, the population in coastal and delta zones is projected to increase
65 in all Shared Socioeconomic Pathways (SSPs) by 2050, with especially the population living in the low elevated coastal zone projected to exceed one billion (by 2050) in all SSPs (Merkens et al., 2016) and likely to reach 1.4 billion by 2060 under the high end growth assumption (Neumann et al., 2015). Increases in population inevitably increase water demand, which is often



satisfied by excessive groundwater extraction, which, more often than not, leads to land subsidence, further exacerbating the flood hazard (due to increased inundation levels). The combination of increased flood hazard and increased population/infrastructure will, in turn, lead to an increase in flood risk in these vulnerable areas (Nicholls et al., 2007; Lenderink and Van Meijgaard, 2008; Syvitski et al., 2009; Min et al., 2011; Balica et al., 2012; Rojas et al., 2013; Wong et al., 2014; Takagi et al., 2016). However, projections of these trends contain uncertainties. This particularly holds for deltas due to their multi-faceted and dynamic character (Nicholls et al., 2020).

The present study attempts to address the challenge of estimating non-stationary fluvial flood hazard in a way it can inform risk modelling via a computationally efficient modelling approach based on a simplified 1D hydrodynamic model for the entire Mekong Delta (area of 40,577 km²) that is coupled with a detailed 1D/2D coupled model and demonstrates its application at Can Tho city in the Mekong Delta.

2. Essential elements for probabilistic assessment of flood hazards

Robust quantification of flood risk assessment typically requires multiple (thousands of) river and flood model simulations to derive probabilistic flood hazard assessments. This constitutes a major challenge, especially for large river systems, such as the Mekong, due to the associated computational and resource demands. Although the last decade has witnessed a great improvement in computational capabilities and models, traditional modelling approaches still pose significant challenges in terms of computational time required to obtain fully probabilistic flood hazard estimates (McMillan and Brasington, 2007; Neal et al., 2012). Therefore developing computationally efficient modelling approaches to circumvent this particular bottleneck remains an important challenge.

Many studies have attempted to improve the computational performance of 1D and 2D hydraulic models in different ways. These attempts include methods such as:

(i) Model simplification – incorporating simpler representations of the physical processes to reduce the complexity of the model structure, e.g. ignoring certain terms such as inertia to simplify 2D shallow water equation (Bates and De Roo, 2000, Seyoum Solomon et al., 2012); applying Cellular Automata approaches in 1D drainage networks (Austin et al., 2014), and 2D overland flows (Ghimire et al., 2013); using conceptual models (Wolfs et al. 2013; Teng et al., 2015).

(ii) Detail reduction – reducing the level of detail and input details of the model, and/or simulation time-step, e.g. using simplified drainage networks (Davidsen et al., 2017), simplified river networks (Ngo et al., 2018), or lower resolution topographic data (Savage et al., 2016).

(iii) Using superior computational resources: parallel computation in 1D (Burger et al., 2014) and 2D models (Leandro et al., 2014, Zhang et al., 2014), and Cloud computing (Glenis et al., 2013).

These approaches significantly reduce model simulation times (Davidsen et al., 2017; Ngo et al., 2018), especially simplified models. However, simplifying the model also usually reduces the accuracy of the model. The appropriateness of a simplified model should be looked at in terms of the purpose of the intended model application. According to the “fit for purpose model”



100 concept, the choice of a model for flood simulation should be done such that the model that can provide predictions with an acceptable level of accuracy at a reasonable computational time and cost (Wright and Esward, 2013; Haasnoot et al., 2014). In addition to the computational performance of the models, the number of simulations is also a factor influencing the computational cost, especially time consuming 2D simulations. Flood risk assessment in the modern context often calculates flood water levels for different return periods (e.g. 5 yr, 10 yr, 20 yr, 50 yr, 100 yr, etc.). This reduces the number of 2D simulations that need to be executed while still achieving probabilistic flood hazard distributions.

105 Availability of historical data is a factor that influences flood hazard and risk assessment, in terms of flood frequency analysis (Machado et al., 2015; Engeland et al., 2018). Flood frequency analysis is used to determine the peak of flood events corresponding to a specified return period (Bayliss and Reed, 2001) in order to design flood risk reduction measures. However, the length of observed data is not always enough for robust flood frequency analysis. However, synthetic data approaches, such as the synthetic streamflow generator developed by Giuliani et al. (2017), provide to the means to generate a large numbers of time series data based on limited historical data.

110 In summary, key features of an effective non-stationary fluvial flood hazard modelling approach may therefore include (a) model reduction – a substantially simplified 1D model of the river system which can complete a simulation in short time span (e.g. completing a one year simulation of river flow (with hourly time step) in around a minute (Ngo et al., 2018)), (b) strategic use of limited input data (e.g. using a synthetic streamflow generator to generate a large number (e.g. 1000) time series of riverflow based on limited historical data (Giuliani et al., (2017))), (c) reduction of the number of time-consuming 1D/2D coupled model runs required to achieve probabilistic flood hazard results via flood frequency analysis while also considering flood hydrograph patterns, (d) derivation of probabilistic flood hazard quantification. The methodology adopted in this study included all of the above key features, and is summarized in Fig. 1.

120 [Figure 1 about here.]

Model reduction is achieved in this study by gradually reducing the complexity of the detailed 1D model of the river system, using trials with varying levels of complexity. Here the main river artery is retained while systematically removing small and medium tributaries, based on their size and/or distance from the target area (in this case, Can Tho city). In doing this, nodes at essential locations in the river system (e.g. at branching points, places at which the direction of flow changes, locations at which there are large change in river cross-sectional area, etc.) are retained, and nodes at less crucial positions are sequentially removed. After each stage of the model reduction, the model is run for a specific period. The model simulated water levels are compared with the measured water level data at the area of interest to evaluate the accuracy of the model. If the model performance is still good enough, the process of reduction is continued until the simplest level of detail that still provides accurate predictions of water levels in the area of interest is obtained. The final model thus obtained is referred to hereon as the simplified model.

130 In this application, due to limited data availability, the synthetic streamflow generator developed by Giuliani et al. (2017) is used to generate 1000 synthetic river flow time series. Giuliani et al.'s (2017) synthetic streamflow generator combines the



methods of Kirsch et al. (2013) and Nowak et al. (2010), wherein Kirsch's method is used to generate flows on a monthly time step, and Nowak's method is used to disaggregate these monthly flows to a daily time step. This synthetic streamflow generator is available on Github (https://github.com/julianneq/Kirsch-Nowak_Streamflow_Generator). Here, Matlab code is used to generate correlated synthetic historical data at multiple sites, while Python code is used to validate the synthetic historical data statistically (<https://waterprogramming.wordpress.com/2017/08/29/open-source-streamflow-generator-part-i-synthetic-generation/>).

3. Application of the fluvial flood hazard modelling approach in Can Tho, Vietnam

Can Tho (population 1.6 million in 2016) is one of the five cities that are directly administered by the Central Government of Vietnam, and is located in the centre of the Mekong Delta, next to the Hau River (Bassac River) (Fig. 2a). In the coming decades, Can Tho is expected to be a dynamic city not only in the Mekong Delta but also in the entire southern region of Vietnam (Huong and Pathirana. 2013, Mekong Delta Plan. 2013). The city includes five urban districts (Ninh Kieu, Binh Thuy, Cai Rang, O Mon and Thot Not) and four rural districts (Phong Dien, Thoi Lai, Vinh Thanh, Co Do) (Fig. 2b). Situated in a tropical monsoon climate region, Can Tho has two distinct seasons: rainy and dry season. The rainy season usually starts from May and lasts until the end of November, with rainfall during this season accounting for 90 % of the annual rainfall (Can Tho City People's Committee, 2010), while the dry season lasts from December to April with low rainfall. Frequent flooding is a major problem in Can Tho (Huong and Pathirana, 2013; Ngo et al., 2018), at least 2-3 times per year, with inundation depths of up to 50 cm at some places in the city centre. Although Can Tho city is some 80 km upstream from the ocean, it is impacted by tidal water level variations, thus making the city vulnerable to the effects of projected sea-level rise and storm surges. Additionally, Can Tho is already facing many challenges from rapid urbanization, population growth, and poor infrastructure (e.g. city flood drainage network) – all of which combine to increase the city's vulnerability to floods. Figure 3 shows the highest observed flood water levels in Can Tho since 2000 and official flood water level alarms in Can Tho. This study focuses on a part of Ninh Kieu district (population 280,000 in 2019) which is the central area of Can Tho city (Fig. 2c). Ninh Kieu is the most developed district of Can Tho and home to many trade centres, urban areas, and residential areas.

[Figure 2 about here.]

[Figure 3 about here.]

To achieve the goal of producing probabilistic flood hazard estimates for the study area (for the present and 2050), the method adopted here broadly comprised four methodological steps: (a) Model reduction - a substantially simplified 1D model for the entire Mekong Delta developed and validated by Ngo et al. (2018) (b) strategic use of limited input data (seven years data of



river flow) to generate 1000 time series data of river flow at Kratie using the synthetic streamflow generator, (c) reduction of the number of 1D/2D coupled model runs required by flood frequency analysis while also considering the flood hydrograph patterns, and (d) derivation of probabilistic flood hazard quantification for the present and for 2050 under RCP 4.5 and 8.5, with and without land subsidence. The methodology adopted is summarized in Fig. 4. Data sources used for this study are shown in Table 1 and the way in which these data were used here is explained in detail below.

[Figure 4 about here.]

[Table 1 about here.]

3.1 Model reduction

A simplified 1D model for the entire Mekong Delta developed using the open-source dynamic rainfall-runoff simulation model SWMM (Storm Water Management Model, Rossman, 2015) is used to derive the river water levels at Can Tho. First, a detailed SWMM model of the entire Mekong Delta was built based on an existing ISIS model, which comprised 575 nodes and 592 links. Using trials with the varying levels of complexity, nodes and links were systematically removed to arrive at a much reduced SWMM model comprising 37 nodes and 40 links which was able to accurately simulate 1-year of river water levels at Can Tho city in under one minute. The model was calibrated with the year 2000 observed water level data and then validated with the years measured water level data at Chau Doc, Tan Chau and Can Tho gauging stations in 2001, 2002 and 2011 (Ngo et al., 2018). Years 2001 and 2002 are years that typical flood events occurred, while 2011 is a year that an extreme event occurred (on 27th October) (Fig. 3). The simplified model was validated for the 2011 event with the goal of investigating the model's capability to simulate the extreme events, which may occur more often in the future due to Climate change (Panagoulia and Dimou, 1997; Menzel et al., 2002; Prudhomme et al., 2013; Alfieri et al., 2015). The general model performance ratings with respect to the October 2011 event based on two indicators NSE (Nash-Sutcliffe efficiency) and RMAE (Relative Mean Absolute Error) are 0.77 (very good) and 0.04 (excellent), respectively (Ngo et al., 2018).

3.2 Strategic use of limited input data

Upstream boundary condition:

In the application here, seven years (2000 – 2006) of observed flow data at the upper boundary location 'Kratie' were used as forcing for the above described simplified 1D model of the Mekong River. As seven years of data is not sufficient to derive probabilistic results, here a synthetic streamflow generator developed by Giuliani et al. (2017) was used to generate 1000 synthetic flow time series (each one year long) for each scenario in Table 2 (current and future). While it is acknowledged that this approach does not fully replace the utility of long term observational data, due to the probabilistic nature of the streamflow generator, it nevertheless captures the statistical variation of upstream flows compared to simply using the seven years of



available data, which is important in flood hazard modelling.

[Table 2 about here.]

For the future simulations that include the effects of climate change, here we used the annual river discharge projections of
 195 Hoang et al. (2016) under RCP 4.5 and 8.5 as the basis for generating the future river flow data. Hoang et al.'s (2016)
 projections indicate that annual river flow for RCP 4.5 and RCP 8.5 at Kratie in 2050 are expected to change between 3 % to
 8 % and -7 % to 11 %, respectively, relative to the 1971-2000 baseline period adopted in that study. Future river flow data
 were generated by combining the flow of each year in seven years of observed flows used here with a randomly selected %
 change of these projected changes in the flow corresponding to each RCP. Subsequently, the streamflow generator was used
 200 to generate 1000 future riverflow time series (each one year long) corresponding to RCP 4.5 and RCP 8.5.

Downstream boundary condition:

Thirty six years (1979 -2014) of model simulated extreme sea level (tide + surge) data were extracted at the Mekong river
 mouths (Tran De, Ben Trai and An Thuan) from the GTSR data set presented by Muis et al. (2016) to use as the downstream
 boundary condition of the 1D model.
 205 For the future simulations, the above present-day extreme sea levels from the GTSR data were combined with the 2050 regional
 sea level rise projections presented by the Viet Nam Ministry of Nature Resource and Environment (MONRE, 2016) under
 RCP 4.5 and RCP 8.5 for the region containing the aforementioned river mouths. The projected regional sea level rise in the
 area by 2050 (relative to 1986-2005) for RCP 4.5 and RCP 8.5 are 13 to 32 cm and 16 to 35 cm, respectively.
 The simplified 1D model was then executed with one year time series of the above described boundary conditions to generate
 210 river water level at Can Tho. In all, 36,000 simulations were undertaken corresponding with the total number of possible
 combinations of upstream (1000 one-year time series of riverflow) and downstream (36 one-year time series of sea level)
 boundary conditions, resulting in 36,000 water level time series data (each one-year long) at Can Tho per considered scenario
 (current and future).

3.3 Reduction of the number of 1D/2D model runs

215 From the 36,000 one-year long water level time series at Can Tho, the maximum water level of each year in the 36,000
 simulation years was extracted and used to fit an extreme value distribution (Gumbel or Type I). The water level at Can Tho
 corresponding to each return period for each scenario (current or future) was determined based on the fitted Gumbel
 distribution.

Apart from the maximum water levels, it is also important in flood hazard modelling to represent the shape of hydrograph
 220 around the peak water level. To achieve this, here we used a threshold-based method, as is commonly used in flood frequency
 analysis (Lang et al., 1999; Bezak et al., 2014). A threshold value of 2.15m (i.e. maximum measured water level at Can Tho,
 see Fig. 3) was adopted here and annual water level time series (of the full 36,000 series) that contain at least one water level



value exceeding 2.15m were identified. Two distinct flood hydrograph patterns were thus identified and from each of the extreme water level time series corresponding to RCP 4.5 and RCP 8.5 (41 and 162 for RCP 4.5 and RCP 8.5 respectively),
 225 24 h long time series around each peak value (12 h earlier to 12 h later) were extracted.

3.4 Derivation of probabilistic flood hazard quantification

Several different flood parameters can be used to quantify the flood hazard, including inundation level, flow velocity, frequency of flooding, and flood duration, etc. (Ramsbottom et al., 2006; Ward et al., 2011; Moel et al., 2015). Of these, inundation level (water depth) and flow velocity are considered the most important parameters (Penning-Rowsell et al., 1994;
 230 Wind et al., 1999; Merz et al., 2007; Kreibich et al., 2009). However, due to the relatively flat terrain combined with small inundation depths in Can Tho, the effect of the flow velocity is expected to be small compared to that of the flood inundation depth (Dinh et al., 2012). Hence, this study considers inundation levels as the main indicator of the flood hazard in the study area.

To simulate the effect of flood drainage network on flooding in the study area, here we used the detailed 1D urban model
 235 developed for the study area by Huong and Pathirana (2013). This model comprises 479 junctions, 612 conduits, 48 outfalls, and 303 sub-catchments (Fig. 5).

[Figure 5 about here.]

The model parameters were calibrated for the flood event on the 17th of October 2016 based on the observed water depths (at one-minute measurement interval) in the manholes at Nguyen Van Cu and Tran Hung Dao streets (Fig. 5). These are the only
 240 available observed flood water depths in the study area. Here, SWMM5-EA software (Pathirana, 2014), was used to calibrate the most uncertain parameters, i.e. Manning's roughness coefficient of conduits, Manning's roughness coefficient of the previous/imperious surfaces of the sub-catchments and the slope of the sub-catchments. The calibrated 1D urban model was then used to establish an integrated 1D/2D model using PCSWMM software (<http://www.chiwater.com/Software/PCSWMM>). Flood simulations were undertaken for water levels with return periods ranging from 0.5 yr to 100 yr obtained from the flood
 245 frequency analysis described in Section 3.2 for each model scenario in Table 1. A 15 m resolution DEM developed by the Vietnam Institute of Meteorology, Hydrology and Environment was used in all simulations. In the simulations that include land subsidence, a subsidence rate of 1.6 cm/yr was used following Erban et al. (2014) and Minderhoud et al. (2015).

For all model scenarios indicated in Table 1, flood inundation maps were first developed for water level return periods ranging from 0.5 yr to 100 yr (eight inundation maps for each model scenario). The flood maps thus obtained were added into ArcMap
 250 under shapefiles, which were then converted to raster files to extract the maximum inundation depths (during the flood events) corresponding to each return period by using the "Polygon to Raster" tool in Conversion tools of ArcToolbox. Subsequently, maximum inundation depths at all grid cells were aggregated to generate flood hazard maps for each return period.



4 Results and Discussion

Figure 6 shows flood frequency curves at Can Tho for the present, and for 2050 corresponding to RCP 4.5 and RCP 8.5, obtained from the Gumbel distributions that were fitted to the modelled maximum water level at Can Tho based on the results of 1D hydrodynamic model described in Section 3.1.

[Figure 6 about here.]

The water level at Can Tho with return periods ranging from 0.5 yr to 100 yr determined from the above flood frequency analysis for each model scenario are shown in Fig. 7.

[Figure 7 about here.]

The calibration results for the 1D urban drainage model for the flood event of Oct 2016 are shown in Fig. 8. The NSE indicator values between the measured and simulated (present conditions) water depths in the manholes at Nguyen Van Cu and Tran Hung Dao streets is 0.75 (good) and 0.95 (very good), respectively. Thus, the 1D urban drainage model performance for the study area can be considered to be sufficiently accurate.

[Figure 8 about here.]

Figure 9 shows the shape of the 24-h time series of all the modelled extreme water level (i.e. peaks greater than the threshold value of 2.15 m) time series at Can Tho (of all 36,000 annual time series) corresponding to RCP 4.5 and RCP 8.5. There are at least two dominant hydrograph shapes in the two RCPs considered (indicated by Pattern 1 and Pattern 2 in Fig. 9a and Fig. 9b), but it is clearer in RCP 8.5. Hence, the response of different river water level hydrographs on flooding was examined, with results (Fig. 10) indicating that flood extent and inundation depths associated with Pattern 1 are greater than that associated with Pattern 2. The inundated area (for cells with maximum inundation depths $\geq 0.02\text{m}$) corresponding to 100-year return period water level for RCP 4.5 and RCP 8.5 with Pattern 1 are 1.96 km^2 and 2.30 km^2 , respectively. The corresponding flooded areas for Pattern 2 are lower at 1.41 km^2 and 1.81 km^2 . Therefore, in this study, 24-h boundary condition time series for the 1D/2D flood model for each modelled scenario was created by combining the calculated water levels corresponding to each return period and a typical river water level time series following Pattern 1. This was a necessary simplification to reduce the complexity and computational burden of computing flood inundation.

[Figure 9 about here.]

[Figure 10 about here.]

Figures 11-13 show flood hazard maps corresponding to 0.5, 5, 50, 100 yr return period water levels (at Can Tho) for the present (model scenario #1), and 2050 under RCP 4.5 and RCP 8.5 (without land subsidence) (model scenarios #3 and #5



respectively). The remaining flood hazard maps which correspond to 1, 2, 10, 20 yr return period water levels for these scenarios are shown in the Appendix A (Figs. A1-A3).

[Figure 11 about here.]

[Figure 12 about here.]

285 [Figure 13 about here.]

[Figure 14 about here.]

Figures 11a and 14 show that, under present conditions, 4.9 % of the study area will be flooded even with the 0.5 yr return period water level at Can Tho, especially some areas along the canals and lakes in the city that are connected to the Can Tho River and Cai Khe channel. Notably, there is a large area of Cai Khe ward (shown by the red circle of Fig. 11a), which is located close to the junction of Hau river, Can Tho river and Cai Khe channel (see Fig. 2c) that is inundated under this condition.

At the other higher end of the modelled return periods under present conditions, Figs. 11d and 14 show that the inundated area with a 100 yr return period water level at Can Tho, is more than double that with a 0.5 yr return period water level at Can Tho increasing from 4.9 % (0.5 yr RP) to 12.7 % (100 yr RP), see Fig. 14).

295 For the future modelled scenarios (without land subsidence; model scenarios #3 and #5), the % inundated areas for the 100 yr RP water level at Can Tho are 29.2 % and 34.2 %, under RCP 4.5 and RCP 8.5 respectively, representing more than a doubling of the inundated area by 2050, relative to the present.

Flood hazard maps corresponding to 0.5, 5, 50, 100 yr return period water levels (at Can Tho) for the future scenarios (2050 - under RCP 4.5 and RCP 8.5) that do take into account land subsidence (model scenarios #2 and #4) are shown in Figs. 15 and 300 16. The remaining flood hazard maps which correspond to 1, 2, 10, 20 yr return period water levels for these scenarios are shown in the Appendix A (Figs. A4 and A5). The difference is immediately visible with a large increase in the flood hazard compared to when land subsidence is not taken into account.

[Figure 15 about here.]

[Figure 16 about here.]

305 [Figure 17 about here.]

Figures 15 and 16 both show severe flooding in a vast majority of the study area for all return periods of water level. The



percentage area flooded by the 0.5 yr RP water level under RCP 4.5 and RCP 8.5 are 73.4 % and 75.3 % respectively (Fig. 17), almost a 10-fold increase relative the comparable projections without land subsidence and a 15-fold increase relative to present-day flooding due to the same RP water level. For the 100 yr RP water level, the percentage area flooded under RCP 4.5 and RCP 8.5 projected to be 95.2 % and 96.4 % respectively, representing a 3-fold increase relative to the comparable projections without land subsidence and a 8-fold increase relative to present-day flooding by the same RP water level. It is also noteworthy that the maximum inundation depths for the 100-year return period water level under RCP 4.5 and 8.5 are not much different at 3.17 m, and 3.20 m, respectively.

The above results highlight that while climate change will increase the flood hazard in the study area, land subsidence has a much greater effect than climate change driven variations in river flow on the flood hazard in the study area. Furthermore, clearly, the existing urban drainage network is not able to effectively drain flood waters even for present-day conditions, and this will be felt more severely in the coming decades. A significant reduction in groundwater extraction, which is the main cause of land subsidence in Can Tho (Erban et al., 2014) combined with a new and substantially efficient urban drainage network may be able to mitigate the projected flood hazard in the study area. It is recommended that the efficacy of these mitigation measures be investigated in detail in future modelling studies.

5 Conclusions

An efficient modelling approach that combines a simplified 1D hydrodynamic model with a detailed 1D/2D coupled model was developed and demonstrated at Can Tho city in the Mekong Delta. Key features of the modelling approach include (a) Model reduction - a substantially simplified 1D model for the entire Mekong Delta (area of 40,577 km²) which can simulate one year of riverflow (with an hourly time step) in under 60 seconds, (b) strategic use of limited input data (seven years data of river flow) to generate 1000 time series data of river flow at Kratie using the synthetic streamflow generator, (c) reduction of the number of 1D/2D coupled model runs required by performing flood frequency analysis while also considering flood hydrograph patterns, and (d) derivation of probabilistic flood hazard quantification for the present and for 2050 under RCP 4.5 and 8.5, with and without land subsidence. The detailed 1D/2D coupled model was successfully validated against measured flood depths at two locations during the Oct 2016 flood event.

Flood hazard maps showing the maximum inundation depth during a flood event were developed for water level return periods ranging from 0.5 yr to 100 yr. Analysis of the flood hazard maps indicate that even under present conditions, more than 12 % of the study area will be inundated by the 100 yr return period water level. With climate change, but without land subsidence, the 100 yr return period flood extent is projected to more than double by 2050, with not much of difference between the two climate scenarios considered (RCP 4.5 and RCP 8.5). However, if the present rate of land subsidence will continue in the future, by 2050 and under both RCP 4.5 and RCP 8.5, the 0.5 yr and 100 yr return period flood extents are projected to increase by around 15-fold and 8-fold respectively, relative to the present-day flood extent.

These results indicate that reducing the rate of land subsidence, for example, by limiting ground water extraction, would



substantially mitigate future flood hazards in the study area. Combining such a measure with a new and more efficient urban
340 drainage network would further reduce the flood hazard. Future modelling studies are needed to quantitatively assess the
hazard and risk reduction afforded by these adaptation measures, which could directly feed into to risk informed adaptation
measures and pathways. For Can Tho, the “do-nothing” management option does not appear to be an option given especially
the 15-fold increase in flood extent projected by 2050 for even the twice per year (0.5 yr return period) flood event.

345

350

355



360 Appendix A

[Figure A1 about here.]

[Figure A2 about here.]

[Figure A3 about here.]

[Figure A4 about here.]

365 [Figure A5 about here.]

Author contribution: HN, AP and RR conceptualized the study. EK extracted modelled surge and tide levels at the Mekong river mouths. DM assisted with SWMM modelling. HN collated the data, did all the modelling and analysis of results with the guidance of AP and RR. All authors contributed to preparing the manuscript.

370 **Competing interests:** The authors declare no conflict of interest. The funding sponsors had no role in the design of the study; in the collection, analyses, or interpretation of data; in the writing of the manuscript, or in the decision to publish the results.

Acknowledgements: HN is supported by IHE Delft projects OPTIRISK, DURA FR Research fund, and AXA CC&CR. RR is supported by the AXA Research fund and the Deltares Strategic Research Programme ‘Coastal and Offshore Engineering’.

375 The authors would like to thank CHI (Computational Hydraulics International) for providing the PCSWMM licence and SURFsara for giving the grant to use the e-infra/SURFsara HPC Cloud.

References

- Alfieri, L., Burek, P., Dutra, E., Krzeminski, B., Muraro, D., Thielen, J., and Pappenberger, F.: GloFAS – global ensemble streamflow forecasting and flood early warning, *Hydrol. Earth Syst. Sci.*, 17, 1161–1175, doi:10.5194/hess-17-1161-2013, 380 2013.
- Alfieri, L., Burek, P., Feyen, L., and Forzieri, G.: Global warming increases the frequency of river floods in Europe, *Hydrol. Earth Syst. Sci.*, 19, 2247–2260, https://doi.org/10.5194/hess-19-2247-2015, 2015.
- Alfieri, L., Bisselink, B., Dottori, F., Naumann, G., Wyser, K., Feyen, L. and Roo, A. De.: Future Global projections of river



- flood risk in a warmer world, *Earth's Future*, doi:10.1002/2016EF000485, 2017.
- 385 Arnell, N. W. and Gosling, S. N.: The impacts of climate change on river flood risk at the global scale, *Clim. Change.*, 134, 387–401, doi:10.1007/s10584-014-1084-5, 2016.
- Austin, R. J., Chen, A. S., Savić, D. A. and Djordjević, S.: Quick and accurate Cellular Automata sewer simulator, *J. Hydroinformatics*, 16(6), 1359–1374, doi:10.2166/hydro.2014.070, 2014.
- Bates, P.D., De Roo, A.P.J.: A simple raster-based model for flood inundation simulation, *J. Hydroinformatics*. 236 (1), 54–
 390 77, 2000.
- Balica, S., Dinh, Q., Popescu, I., Vo, T. Q., Pham, D. Q.: Flood impact in the Mekong Delta, Vietnam, *J. Maps.*, 0(0), 1–12, doi:10.1080/17445647.2013.859636, 2014.
- Balica, S.F., Wright, N.G. and van der Meulen, F. A flood vulnerability index for coastal cities and its use in assessing climate change impacts, *Nat Hazards.*, 64, 73–105, doi:10.1007/s11069-012-0234-1, 2012.
- 395 Burger, G., Sitzenfrie, R., Kleidorfer, M. and Rauch, W.: Parallel flow routing in SWMM 5, *Environ. Model. Softw.*, 53, 27–34, doi:10.1016/j.envsoft.2013.11.002, 2014.
- Bezak, N., Brilly, M. and Šraj, M.: Comparison between the peaks-over-threshold method and the annual maximum method for flood frequency analysis, *Hydrol. Sci. J. – J. des Sci. Hydrol.*, 59(5), 959–977, doi:10.1080/02626667.2013.831174, 2014.
- Can Tho City People's Committee: Can Tho City Climate Change Resilience Plan, 2010.
- 400 Chen, R., Zhang, Y., Xu, D., Liu, M.: Climate Change and Coastal Megacities: Disaster Risk Assessment and Responses in Shanghai City, in: *Climate Change, Extreme Events and Disaster Risk Reduction. Sustainable Development Goals Series*, edited by: Mal, S., Singh, R., Huggel, C., Springer, Cham, doi:10.1007/978-3-319-56469-2_14, 2018.
- Moel, H. De, Jongman, B., Kreibich, H. and Merz, B.: Flood risk assessments at different spatial scales, 865–890, doi:10.1007/s11027-015-9654-z, 2015.
- 405 Davidsen, S., Löwe, R., Thrysøe, C. and Arnbjerg-Nielsen, K.: Simplification of one-dimensional hydraulic networks by automated processes evaluated on 1D/2D deterministic flood models, *J. Hydroinformatics*, 19(5), 686–700, doi:10.2166/hydro.2017.152, 2017.
- Dinh, Q., Balica, S., Popescu, I., Jonoski, A.: Climate change impact on flood hazard, vulnerability and risk of the Long Xuyen Quadrangle in the Mekong Delta Climate change impact on flood hazard, vulnerability and risk of the Long Xuyen, *Int. J. River Basin Manag.*, 10, 103–120, doi:10.1080/15715124.2012.663383, 2012.
- 410 Erban, L. E., Gorelick, S. M. and Zebker, H. A.: Groundwater extraction, land subsidence, and sea-level rise in the Mekong Delta, Vietnam, *Environ. Res. Lett.*, 9, doi:10.1088/1748-9326/9/8/084010, 2014.
- Forzieri, G., Cescatti, A., Batista, F. and Feyen, L.: Articles Increasing risk over time of weather-related hazards to the European population: a data-driven prognostic study, *Lancet Planet Heal.*, 1(5), e200–e208, doi:10.1016/S2542-
 415 5196(17)30082-7, 2017.
- Foudi, S., Osés-eraso, N. and Tamayo, I.: Integrated spatial flood risk assessment: The case of Zaragoza Land Use Policy Integrated spatial flood risk assessment, 42, 278–292, doi:10.1016/j.landusepol.2014.08.002, 2015.



- Giuliani, M., Quinn, J. D., Herman, J. D., Castelletti, A., & Reed, P. M.: Scalable multiobjective control for large-scale water resources systems under uncertainty, *IEEE Transactions on Control Systems Technology*, 26(4), 1492–1499, doi: 10.1109/TCST.2017.2705162, 2017.
- Ghimire, B., Chen, A. S., Guidolin, M., Keedwell, E. C., Djordjević, S. and Savić, D. A.: Formulation of a fast 2D urban pluvial flood model using a cellular automata approach, *J. Hydroinformatics*, 15(3), 676–686, doi:10.2166/hydro.2012.245, 2013.
- Glenis, V., McGough, A. S., Kutija, V., Kilsby, C. and Woodman, S.: Flood modelling for cities using Cloud computing, *J. Cloud Comput.*, 2(1), 1–14, doi:10.1186/2192-113X-2-7, 2013.
- Hall, J.W., Dawson, R.J., Sayers, P.B., Rosu, C., Chatterton, J.B., Deakin, R.: A methodology for national-scale flood risk assessment, *Water Maritime Eng.*, 156(3), 235–247, doi:10.1680/maen.156.3.235.37976, 2003.
- Hirabayashi, Y., Mahendran, R., Koirala, S., Konoshima, L., Yamazaki, D., Watanabe, S., Kim, H. and Kanae, S.: Global flood risk under climate change, *Nat. Clim. Chang.*, 3, 4–6, doi:10.1038/nclimate1911, 2013.
- Hoang, L. P., Lauri, H., Kumm, M., Koponen, J., Vliet, M. T. H. Van, Supit, I., Leemans, R., Kabat, P. and Ludwig, F.: Mekong River flow and hydrological extremes under climate change, *Hydrol. Earth Syst. Sci.*, 3027–3041, doi:10.5194/hess-20-3027-2016, 2016.
- Huong, H. T. L. and Pathirana, A.: Urbanization and climate change impacts on future urban flooding in Can Tho city, Vietnam, *Hydrol. Earth Syst. Sci.*, 17(1), 379–394, doi:10.5194/hess-17-379-2013, 2013.
- Kirsch, B. R., Characklis, G. W., & Zeff, H. B.: Evaluating the impact of alternative hydro-climate scenarios on transfer agreements: Practical improvement for generating synthetic streamflows, *J. Water Resour. Plan. Manag.*, 139(4), 396–406, 2012.
- Kreibich, H., Piroth, K., Seifert, I., Maiwald, H., Kunert, U., Schwarz, J., Merz, B. and Thieken, A. H.: Is flow velocity a significant parameter in flood damage modelling?, *Nat. Hazards Earth Syst. Sci.*, 9, 1679–1692, doi: 10.5194/nhess-9-1679-2009, 2009.
- Kundzewicz, Z. W., Kanae, S., Seneviratne, S. I., Handmer, J., Nicholls, N., Peduzzi, P.: Flood risk and climate change: global and regional perspectives, *Hydrol. Sci. J.*, 59, 1–28, doi:10.1080/02626667.2013.857411, 2014.
- Kvočka, D., Falconer, R.A. & Bray, M.: Flood hazard assessment for extreme flood events, *Nat Hazards*, 84, 1569–1599, doi: 10.1007/s11069-016-2501-z, 2016.
- Lang, M., Ouara, T.B.M.J. and Bobée, B.: Towards operational guidelines for over-threshold modeling, *J. Hydrol.*, 225 (3–4), 103–117, doi: 10.1016/S0022-1694(99)00167-5, 1999.
- Leandro, J., Chen, A. S. and Schumann, A.: A 2D parallel diffusive wave model for floodplain inundation with variable time step (P-DWave), *J. Hydrol.*, 517, 250–259, doi:10.1016/j.jhydrol.2014.05.020, 2014.
- Lenderink, G. and Meijgaard, E. V. A. N.: Increase in hourly precipitation extremes beyond expectations from temperature changes, *Nat Geosci.*, 511–514, doi:10.1038/ngeo262, 2008.



- McMillan, H.K. and Brasington J.: Reduced complexity strategies for modelling urban floodplain inundation, *Geomorphology*, 90, 226–243, 2007.
- Menzel, L., Niehoff, D., Bürger, G., Bronstert, A.: Climate change impacts on river flooding: a modelling study of three meso-scale catchments, in: *Climatic Change: Implications for the Hydrological Cycle and for Water Management*, edited by: Beniston, M., Springer, Netherlands, pp. 249–269, doi: 10.1007/0-306-47983-4_14, 2002.
- 455 Merkens, J., Reimann, L., Hinkel, J. and Vafeidis, A. T.: Gridded population projections for the coastal zone under the Shared Socioeconomic Pathways, *Glob. Planet. Change*, 145, 57–66, doi:10.1016/j.gloplacha.2016.08.009, 2016.
- Merz, B., Thielen, A., Gocht, M.: Flood risk mapping at the local scale: Concepts and Challenges, in: *Flood Risk Management in Europe, Advances in Natural and Technological Hazards Research*, vol 25, edited by: Begum, S., Stive, M.J.F., Hall, J.W., Springer, Dordrecht, 231–251, doi: 10.1007/978-1-4020-4200-3_13, 2007.
- 460 Merz, B., Hall, J., Disse, M., and Schumann, A.: Fluvial flood risk management in a changing world, *Nat. Hazards Earth Syst. Sci.*, 10, 509–527, doi:10.5194/nhess-10-509-2010, 2010.
- Meyer, V., Haase, D., Scheuer, S.: Flood risk assessment in European river basins--concept, methods, and challenges exemplified at the Mulde River, *Integr Environ Assess Manag.*, 5(1), 17–26, doi:10.1897/ieam_2008-031.1, 2009.
- 465 Min, S-K., Zhang, X., Zwiers, F.W., Hegerl, G.C.: Human contribution to more-intense precipitation extremes, *Nature.*, 470(7334), 378–381, doi:10.1038/nature09763, 2011.
- Minderhoud, P. S. J., Erkens, G., Pham, V. H., Vuong, B. T. and Stouthamer, E.: Assessing the potential of the multi-aquifer subsurface of the Mekong Delta (Vietnam) for land subsidence due to groundwater extraction, *Proc. Int. Assoc. Hydrol. Sci.*, 372, 73–76, doi:10.5194/piahs-372-73-2015, 2015.
- 470 Mishra, K. and Sinha, R.: Geomorphology Flood risk assessment in the Kosi megafan using multi-criteria decision analysis : A hydro-geomorphic approach, *Geomorphology*, 350, 106861, doi:10.1016/j.geomorph.2019.106861, 2020.
- Moel, H. De, Jongman, B., Kreibich, H. and Merz, B.: Flood risk assessments at different spatial scales, *Mitig Adapt Strateg Glob Change.*, 865–890, doi:10.1007/s11027-015-9654-z, 2015.
- MONRE.: *Climate Change and Sea Level Rise Scenarios for Vietnam*, Ministry of Natural Resources and Environment, Hanoi, Vietnam, 2016.
- 475 Mora, C., Spirandelli, D., Franklin, E. C., Lynham, J., Kantar, M. B., Miles, W., Smith, C. Z., Freel, K., Moy, J., Louis, L. V., Barba, E. W., Bettinger, K., Frazier, A. G., Ix, J. F. C., Hanasaki, N., Hawkins, E., Hirabayashi, Y., Knorr, W., Little, C. M. and Emanuel, K.: hazards intensified by greenhouse gas emissions, *Nat. Clim. Chang.*, doi:10.1038/s41558-018-0315-6, 2018.
- Mosavi, A.; Ozturk, P.; Chau, K.-W.: Flood Prediction Using Machine Learning Models: Literature Review, *Water.*, 10, doi:10.3390/w10111536, 2018.
- 480 Muis, S., Verlaan, M., Winsemius, H.C., Aerts, J. C. J. H., Ward, P. J.: A global reanalysis of storm surges and extreme sea levels, *Nat Commun.*, doi:10.1038/ncomms11969, 2016.
- Neal, J., Villanueva, I., Wright, N., Willis, T., Fewtrell, T. and Bates, P.: How much physical complexity is needed to model flood inundation ?, *Hydrol. Processes*, 26, 2264–2282, doi:10.1002/hyp.8339, 2012.



- 485 Neumann, B., Vafeidis, A. T., Zimmermann, J. and Nicholls, R. J.: Future Coastal Population Growth and Exposure to Sea-Level Rise and Coastal Flooding - A Global Assessment, *PLoS One.*, 10(6), doi:10.1371/journal.pone.0118571, 2015.
- Ngo, H., Pathirana, A., Zevenbergen, C., Ranasinghe, R.: An Effective Modelling Approach to Support Probabilistic Flood Forecasting in Coastal Cities – Case Study: Can Tho, Mekong Delta, Vietnam, *J. Mar. Sci. Eng.*, 1–19, doi:10.3390/jmse6020055, 2018.
- 490 Nicholls, R.J.: Coastal Flooding and Wetland Loss in the 21st Century: Changes under the SRES Climate and Socio-Economic Scenarios, *Global Environmental Change.*, 14, 69–86, doi: 10.1016/j.gloenvcha.2003.10.007, 2004.
- Nicholls, R. J.; Wong, P. P.; Burkett, V.; Codignotto, J.; Hay, J.; McLean, R.; Ragoonaden, S.; Woodroffe, C. D.; Abuodha, P. A. O.; Arblaster, J.; Brown, B.; Forbes, D.; Hall, J.; Kovats, S.; Lowe, J.; McInnes, K.; Moser, S.; Rupp-Armstrong, S.; and Saito, Y.: Coastal systems and low-lying areas, 2007.
- 495 Nicholls, R.J.; Adger, W.N.; Hutton, C.W.; Hanson, S.E.: Delta Challenges and Trade-Offs from the Holocene to the Anthropocene, in: *Deltas in the Anthropocene*, edited by: Nicholls, R., Adger, W., Hutton, C., Hanson, S., Palgrave Macmillan, Cham, UK, doi:10.1007/978-3-030-23517-8_1, 2020.
- Nowak, K., Prairie, J., Rajagopalan, B. and Lall, U.: A nonparametric stochastic approach for multisite disaggregation of annual to daily streamflow, *Water Resour. Res.*, 46(8), doi:10.1029/2009WR008530, 2010.
- 500 Panagouliaas, D. and Dimoub, G.: Sensitivity of flood events to global climate change, *J. Hydrol.*, 1694, 208–222, 1997.
- Pappenberger, F., Dutra, E., Wetterhall, F. and Cloke, H. L.: Deriving global flood hazard maps of fluvial floods through a physical model cascade, *Nat Hazards Earth Syst Sci.*, 4143–4156, doi:10.5194/hess-16-4143-2012, 2012.
- Pasquier, U., He, Y., Hooton, S., Goulden, M. and Hiscock, K. M.: An integrated 1D–2D hydraulic modelling approach to assess the sensitivity of a coastal region to compound flooding hazard under climate change, *Nat. Hazards*, 98(3), 915–937, doi:10.1007/s11069-018-3462-1, 2019.
- 505 Pathirana, A.: SWMM5-EA-A tool for learning optimization of urban drainage and sewerage systems with genetic algorithms. In *Proceedings of the 11th International Conference on Hydroinformatics*, New York, NY, USA, 17–21 August 2014; CUNY Academic Works: New York, NY, USA, 2014.
- Penning-Rowsell, E. C., Fordham, M., Correia, F. N., Gardiner, J., Green, C., Hubert, G., Ketteridge, A.-M., Klaus, J., Parker, D. Peerbolte, B., Pflugner, W., Reitano, B., Rocha, J., Sanchez- Ar-cilla, A., Saraiva, M. d. G., Schmidtke, R., Torterotot, J.-P., van der Veen, A., Wierstra, E., and Wind, H.: Flood hazard assessment, modelling and management: Results from the EUROflood project, in *Floods across Europe: Flood hazard assessment, modelling and management*, edited by: Penning-Rowsell, E. C., and Fordham, M., Middlesex University Press, London, 1994.
- 510 Penning-Rowsell, E., Floyd, P., Ramsbottom, D., Surendran, S.: Estimating injury and loss of life in floods: a deterministic framework, *Nat Hazards.*, 36:43–64, doi: 10.1007/s11069-004-4538-7, 2005.
- Prudhomme, C., Crooks, S. and Kay, A. L.: Climate change and river flooding : Part 1 Classifying the sensitivity of British catchments Climate change and river flooding : part 1 classifying the sensitivity of British catchments, *Clim. Change.*, doi:10.1007/s10584-013-0748-x, 2013.



- Ramsbottom, D., Floyd, P., Penning-Rowsell, E.: Flood risks to people: Phase 1. R&D Technical Report FD2317, Department for the Environment, Food and Rural Affairs (DEFRA), UK Environment Agency, 2003.
- Ranasinghe, R. and Jongejan, R.: Climate Change, Coasts and Coastal Risk, *J. Mar. Sci. Eng.*, 6–9, doi:10.3390/jmse6040141, 2018.
- Rojas, R., Scientific, T. C. and Watkiss, P.: Climate change and river floods in the European Union : Socio-economic consequences and the costs and benefits of adaptation, *Glob Environ Change*, 1737–1751, doi:10.1016/j.gloenvcha.2013.08.006, 2013.
- Rossman, L.A.: Storm Water Management Model User’s Manual, EPA, Cincinnati, OH, USA, pp. 1–353, 2015.
- Bureau Reclamation: <https://www.usbr.gov/ssle/damsafety/risk/methodology.html>, last access: 11 May, 2020.
- Savage, J. T. S., Bates, P., Freer, J., Neal, J., & Aronica, G. T.: When does spatial resolution become spurious in probabilistic flood inundation predictions? *Hydrological Processes*, 30(13), 2014–2032, <https://doi.org/10.1002/hyp.10749>, 2016.
- Small, C., and Nicholls, R.: A global analysis of human settlement in coastal zones, *J. Coast Res.*, 19, 584–599, 2003.
- Seyoum Solomon, D., Vojinovic, Z., Price Roland, K., Weesakul, S.: Coupled 1D and noninertia 2D flood inundation model for simulation of urban flooding. *J. Hydraul. Eng*, 138 (1), 23–34, 2012.
- Syvitski, J.P.M., Kettner, A.J., Overeem, I., Hutton, E.W.H., Hannon, M.T., Brakenridge, G.R., Day, J., Vörösmarty, C., Saito, Y., Giosan, L., and Nicholls, R.J.: Sinking deltas due to human activities, *Nature Geosci.*, 2, 681–686, doi: 10.1038/ngoe629, 2009.
- Takagi, H., Ty, T. V., Thao, N. D. and Esteban, M.: Ocean tides and the influence of sea-level rise on floods in urban areas of the Mekong Delta, *J. Flood Risk Manage.*, 8, 292–300, doi:10.1111/jfr3.12094, 2015.
- Teng, J., Vaze, J., Dutta, D., Marvanek, S.: Rapid inundation modelling in large floodplains using LiDAR DEM, *Water Resour. Manag*, 29(8):2619–2636, <https://doi.org/10.1007/s11269-015-0960-8>, 2015.
- Valiela, I.: *Global Coastal Change*, Blackwell: Oxford, UK, 368, 2006.
- Ward, P.J., De Moel, H., Aerts, J.C.J.H.: How are flood risk estimates affected by the choice of return-periods? *Nat. Hazards Earth Syst. Sci*, 11, 3181–3195, 2011.
- Wind, H. G., Nieron, T. M., De Blois, C. J., and De Kok, J. L.: Analysis of flood damages from the 1993 and 1995 Meuse floods, *Water Resour. Res.*, 35, 3459–3465, 1999.
- Wolfs, V., Willems, P.: A data driven approach using Takagi-Sugeno models for computationally efficient lumped floodplain modelling. *J. Hydrol*, 503 (Supplement C), 222–232, 2013.
- Wong, P.P., Losada, I.J., Gattuso, J.-P., Hinkel, J., Khattabi, A., McInnes, K.L., Saito, Y., and Sallenger, A.: Coastalsystems and low-lying areas, in: *Climate Change 2014: Impacts, Adaptation, and Vulnerability. Part A: Global and Sectoral Aspects. Contribution of Working Group II to the Fifth Assessment Report of the Intergovernmental Panel on Climate Change*, edited by: Field, C.B., Barros, V.R., Dokken, D.J., Mach, K.J., Mastrandrea, M.D., Bilir, T.E., Chatterjee, M., Ebi, K.L., Estrada, Y.O., Genova, R.C., Girma, B., Kissel, E.S., Levy, A.N., MacCracken, S., Mastrandrea, P.R., and White, L.L., Cambridge University Press, Cambridge, United Kingdom and New York, NY, USA, pp. 361–409, Sallenger, 2014.



Zhang, S., Xia, Z., Yuan, R. and Jiang, X.: Parallel computation of a dam-break flow model using OpenMP on a multi-core computer, J. Hydrol., 512, 126–133, doi:10.1016/j.jhydrol.2014.02.035, 2014.

555

560

565

570

575

580

585

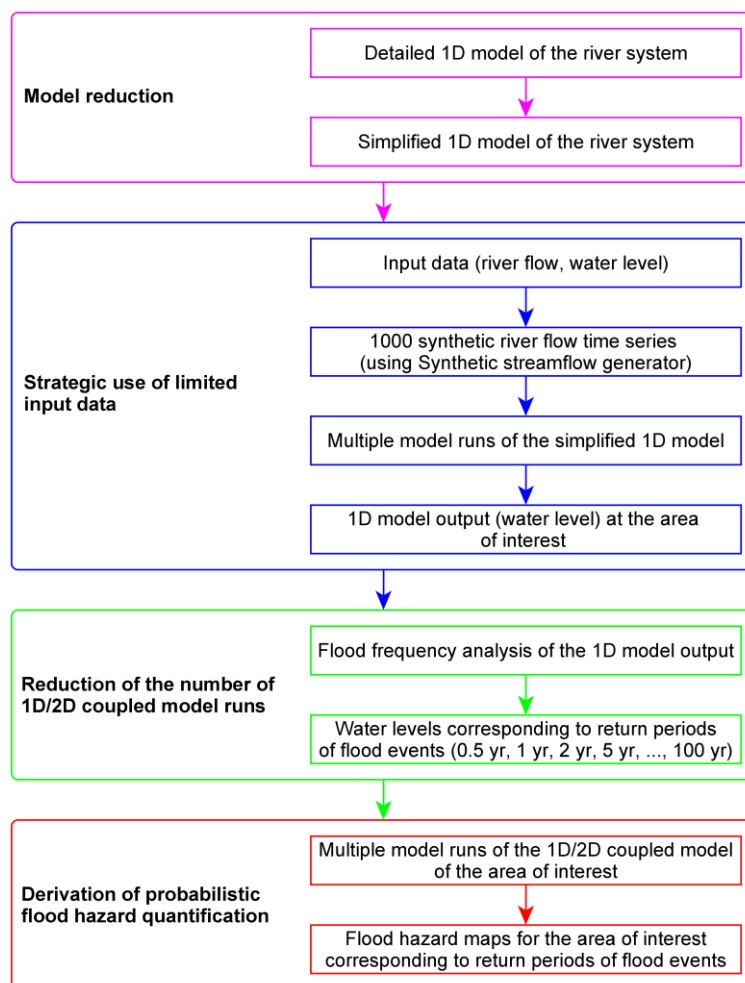


Figure 1: The methodological framework adopted to derive probabilistic flood hazard estimates for the area of interest.

590

595

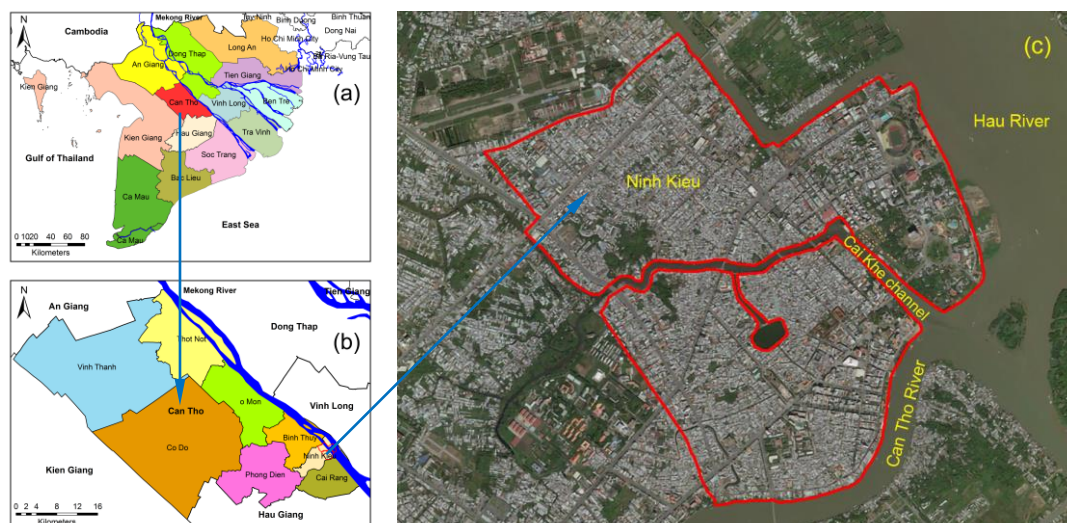


Figure 2: (a) Map of Mekong delta and surrounding provinces, (b) Can Tho city, (c) Study area (bounded by red line) within the Ninh Kieu district in Can Tho city (Base map is from Bing Maps satellite © Microsoft).

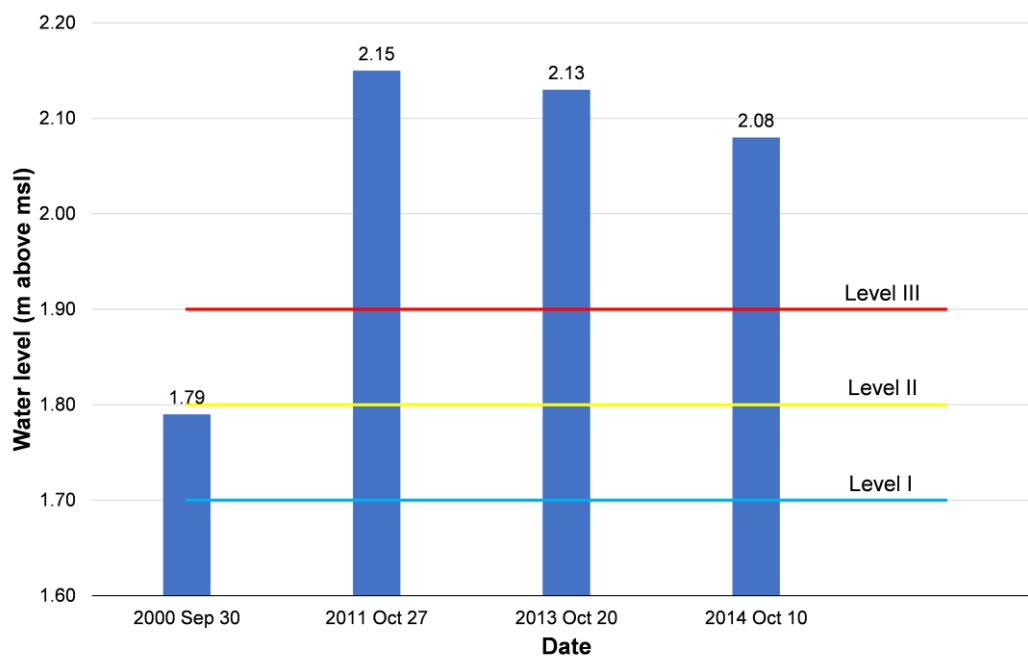


Figure 3: Highest measured water levels of the flooding years since 2000 and flood water level alarms in Can Tho (flood water level alarms are implemented following Decision No.632/QĐ-TTg issued on May 10th, 2010).

625

630

635

640

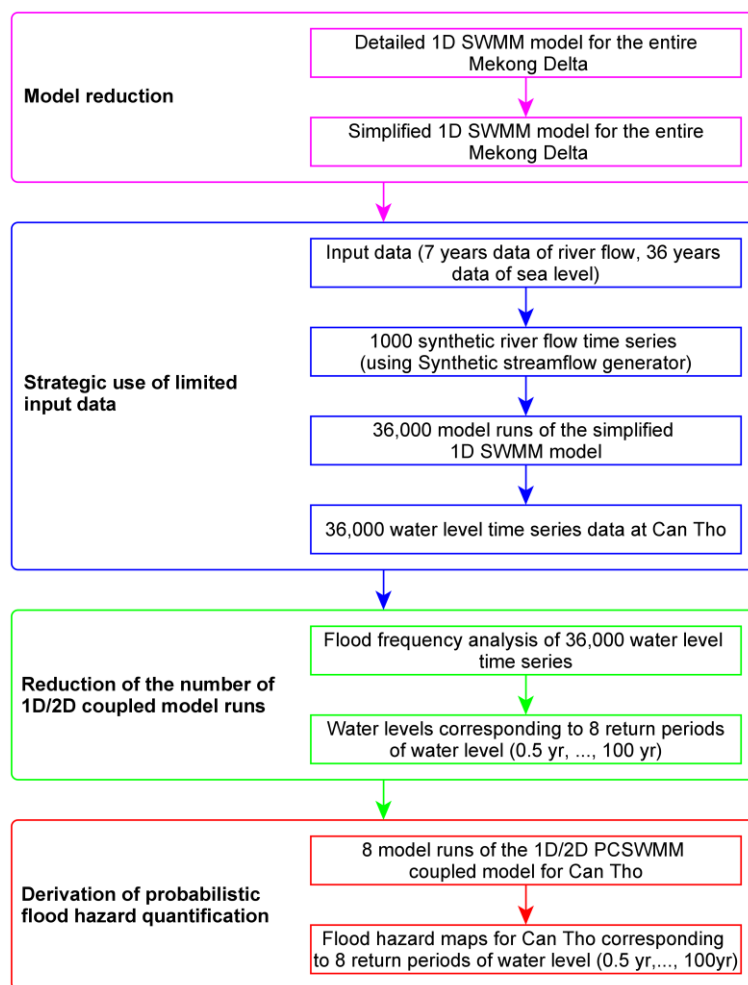
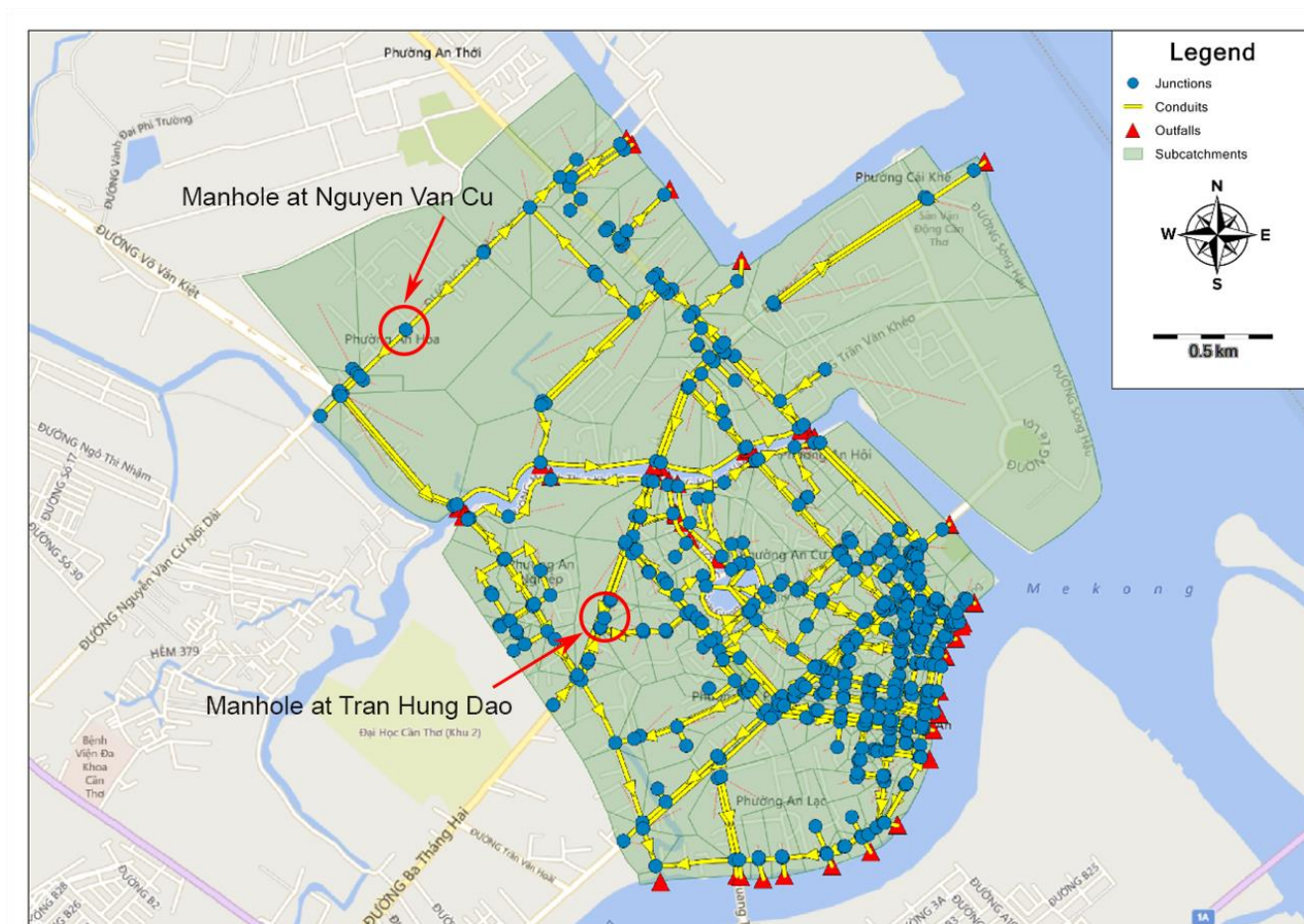


Figure 4: The methodological framework adopted to derive probabilistic flood hazard estimates for the study area. This process was applied for the present and for 2050 (RCP 4.5 and RCP 8.5 together with 3 different local land subsidence scenarios).

645

650



655 **Figure 5: The detailed 1D urban flood drainage model for the study area developed by Huong and Pathirana, (2013) (Base map is**
 660 **from Bing Maps Road © Microsoft).**

660

665

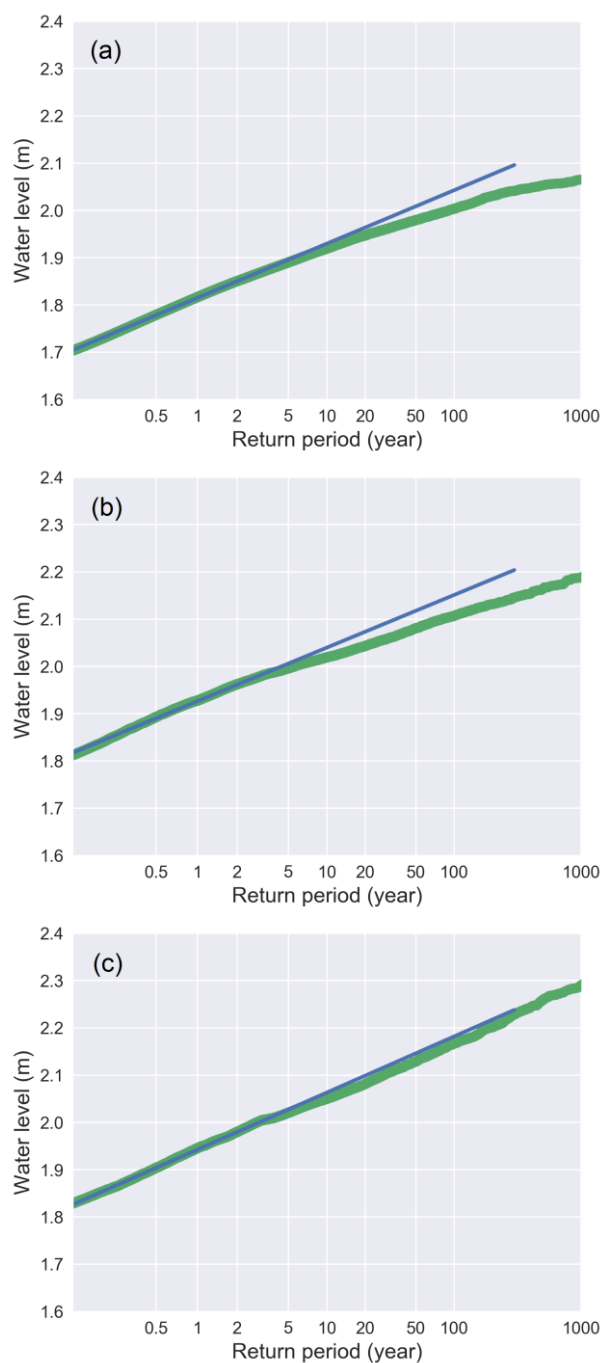


Figure 6: Flood frequency curves at Can Tho for Present (a), and for 2050 corresponding RCP 4.5 (b) and RCP 8.5 (c). Blue line indicates the fitted Gumbel distribution while the green line indicates 1D hydrodynamic model output.

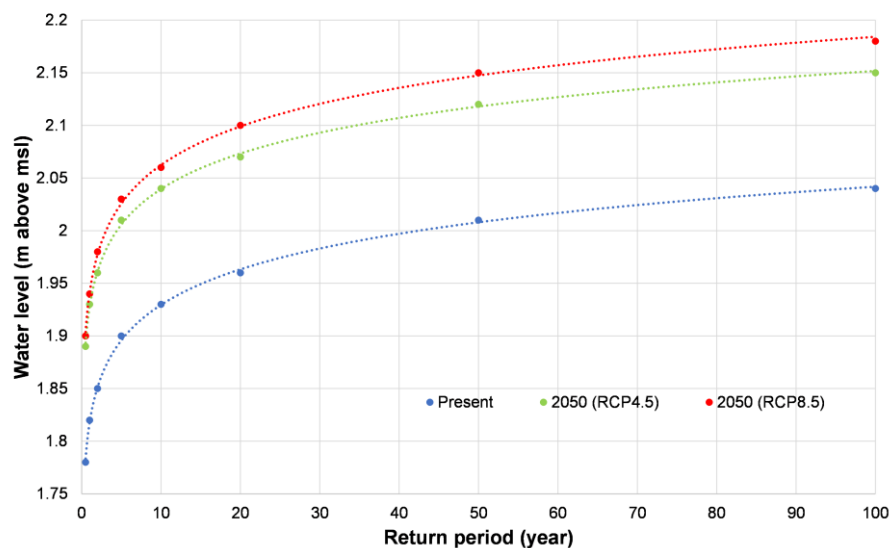


Figure 7: The water level at Can Tho corresponding to each return period for Present, and for 2050 under RCP 4.5 and RCP 8.5.

675

680

685

690

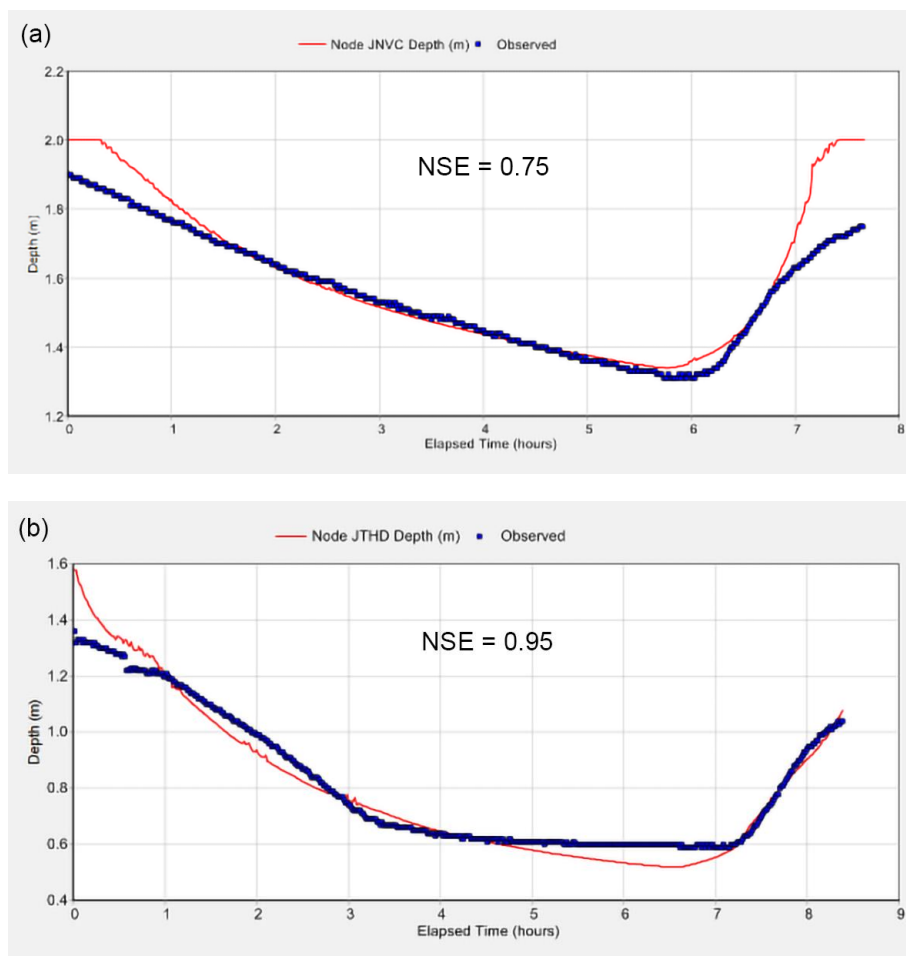


Figure 8: Comparison between simulated and observed water depths in the manholes at Nguyen Van Cu (a) and Tran Hung Dao (b) streets on October 17, 2016.

695

700

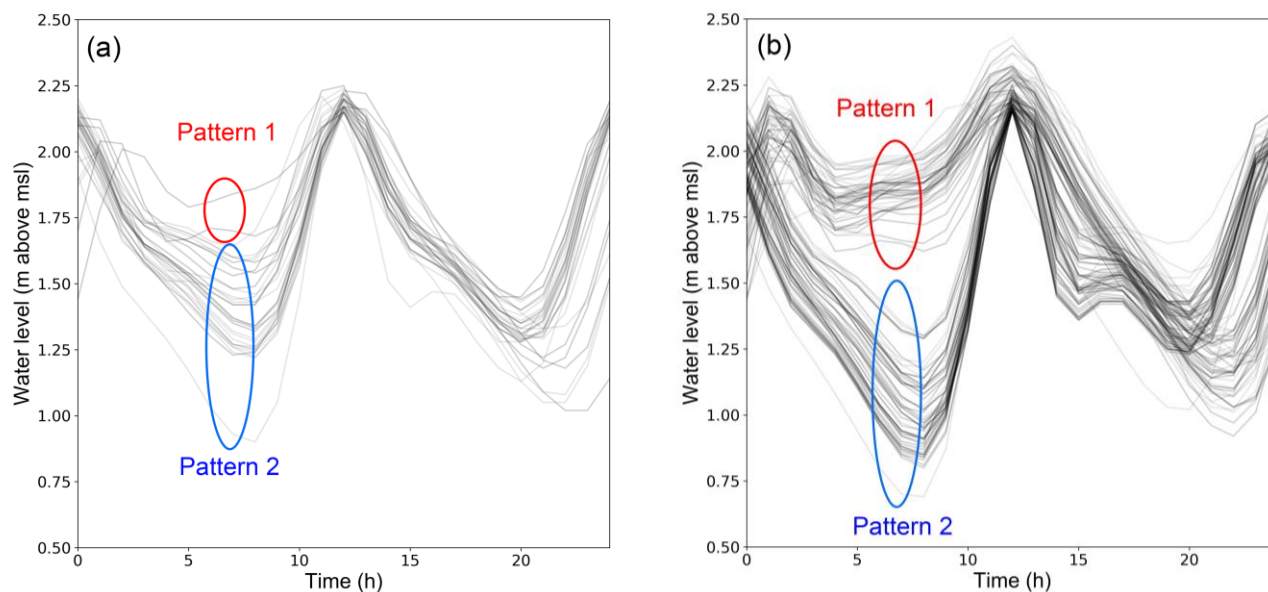


Figure 9: Analysis of 24-h time series around modelled peak water levels indicating two flood hydrograph patterns in the future scenario, (a) – 2050 (RCP4.5), (b) – 2050 (RCP 8.5).

705

710

715

720

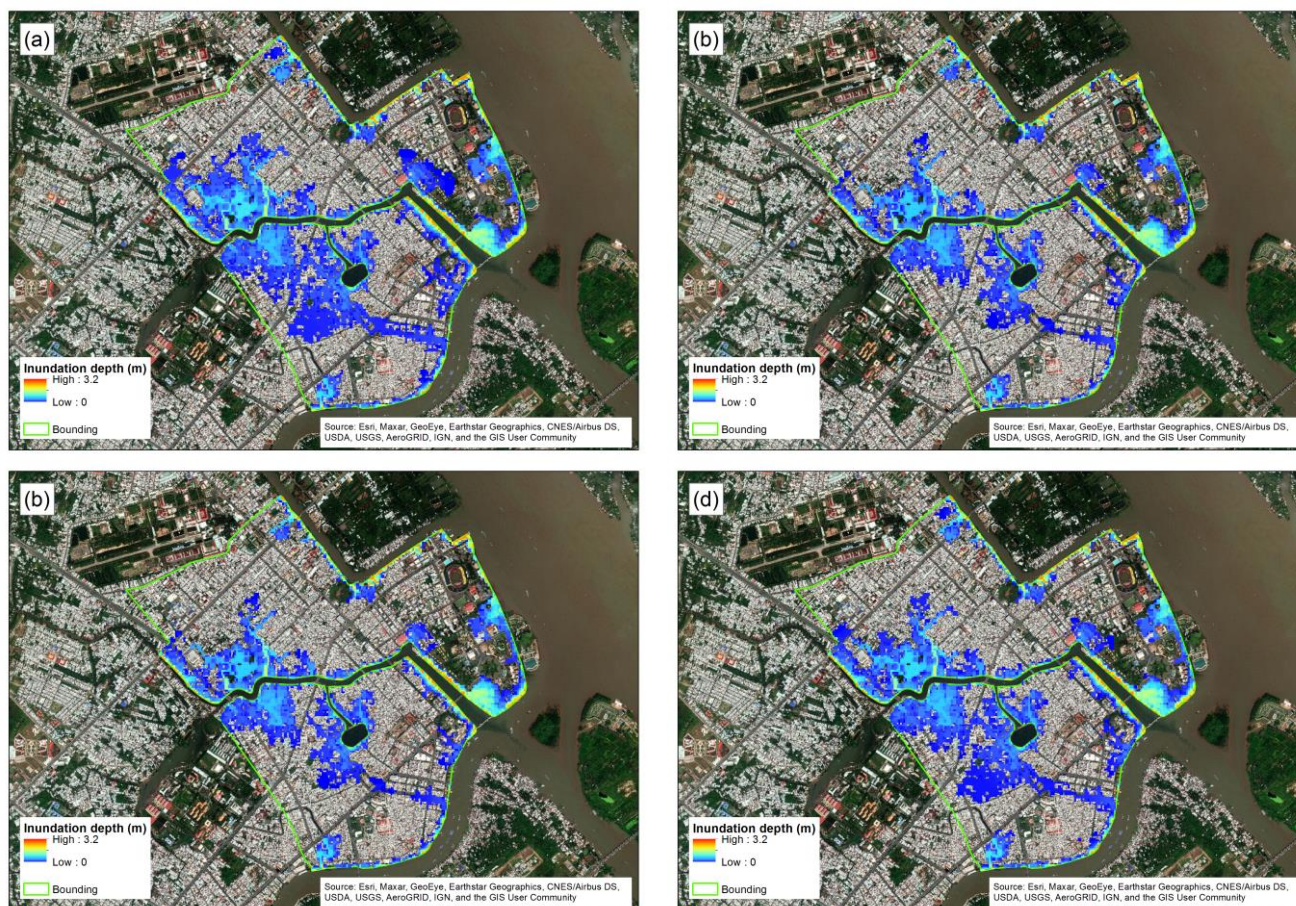


Figure 10: Flood hazard maps (i.e. maximum flood depths) for the 100-year return period of water level for hydrograph Pattern 1 (left) and Pattern 2 (right) under RCP 4.5 (Fig. 9a, Fig. 9b) and RCP 8.5 (Fig. 9c, Fig. 9d) (without land subsidence). The inundated area (for cells with maximum inundation depths $\geq 0.02\text{m}$) for RCP 4.5 and RCP 8.5 corresponding to Pattern 1 are 1.96 km^2 and 2.30 km^2 , respectively, while for Pattern 2 are 1.41 km^2 and 1.81 km^2 , respectively.



Figure 11: Flood hazard maps for the present (model scenario #1) corresponding to each return period of water level, (a) 0.5 yr return period, (b) 5 yr return period, (c) 50 yr return period, (d) 100 yr return period. Red circle in Fig. 11a highlights a large inundated area (present for all return periods) of Cai Khe ward.



Figure 12: Flood hazard maps for 2050 under RCP 4.5 (model scenario #3) corresponding to each return period of water level, (a) 0.5 yr return period, (b) 5 yr return period, (c) 50 yr return period, (d) 100 yr return period.

755

760

765

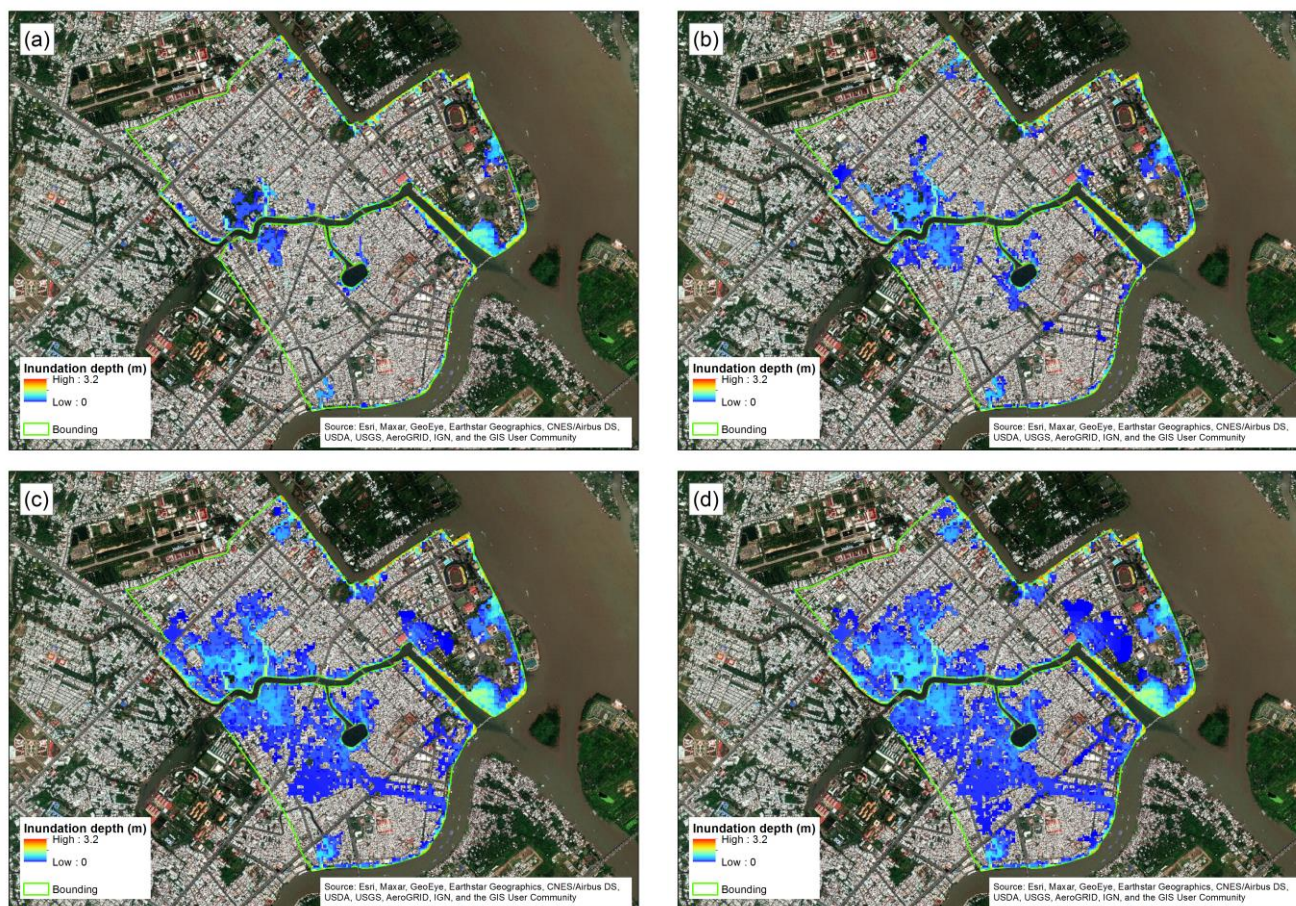


Figure 13: Flood hazard maps for 2050 under RCP 8.5 (model scenario #5) corresponding to each return period of water level, (a) 0.5 yr return period, (b) 5 yr return period, (c) 50 yr return period, (d) 100 yr return period.

770

775

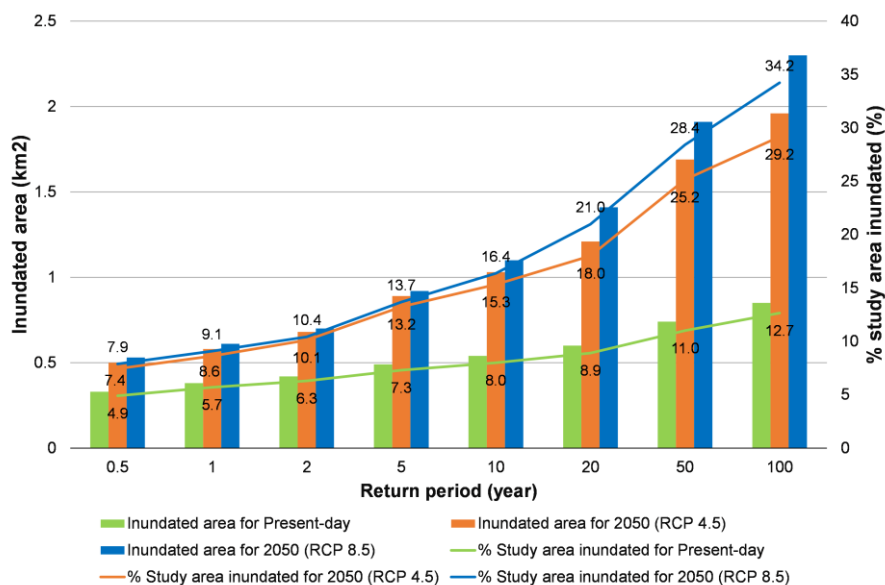


Figure 14: The inundated area and percentage of the flooded area relative to total study area (also indicated by numerics along the solid lines in the figure) corresponding to each return period of water level (without land subsidence).

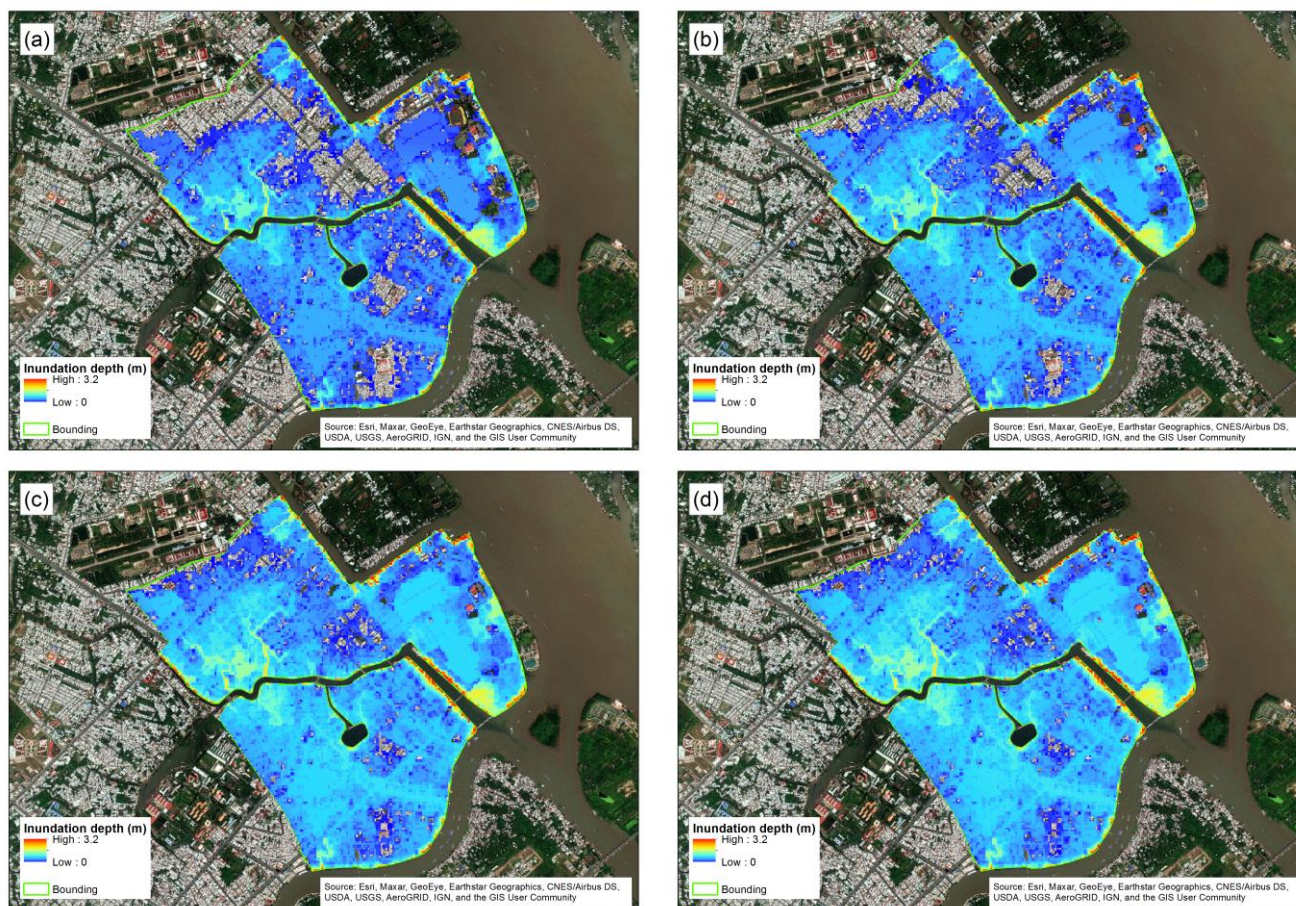


Figure 15: Flood hazard maps for 2050 under RCP 4.5 (model scenario #2) corresponding to each return period of water level, (a) 0.5 yr return period, (b) 5 yr return period, (c) 50 yr return period, (d) 100 yr return period.

800

805

810

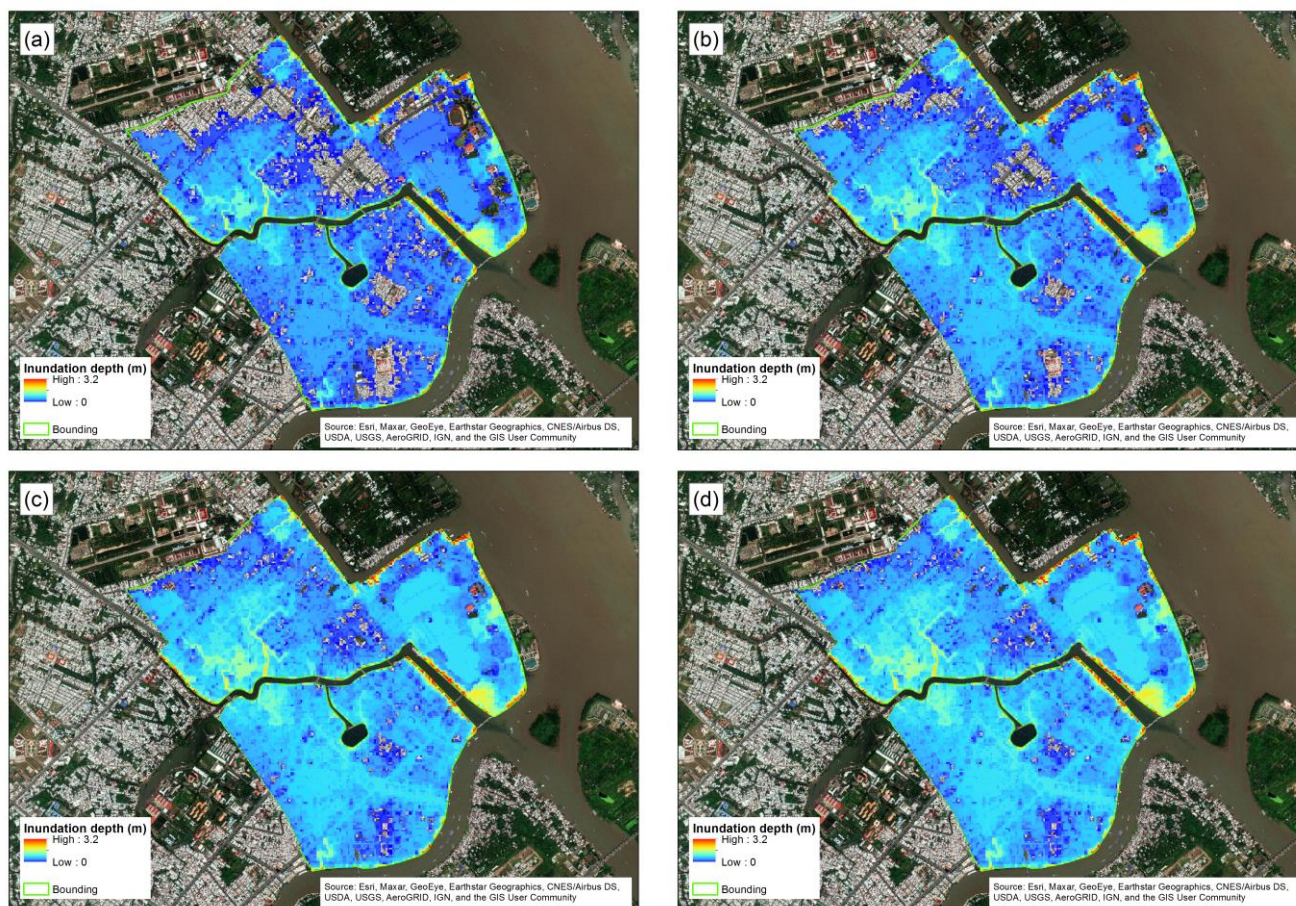
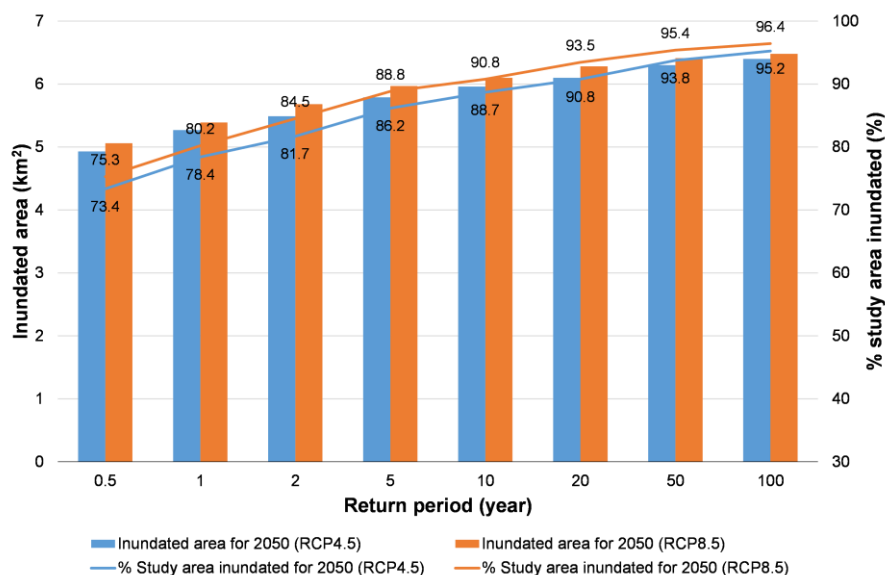


Figure 16: Flood hazard maps for 2050 under RCP 8.5 (model scenario #4) corresponding to each return period of water level, (a) 0.5 yr return period, (b) 5 yr return period, (c) 50 yr return period, (d) 100 yr return period.

815

820



825 **Figure 17: The inundated area and percentage of the flooded area relative to total study area (also indicated by numerics along the**
 830 **solid lines in the figure) corresponding to each return period of water level for model scenarios (including land subsidence).**

830

835

840

845



Figure A1: Flood hazard maps for the present (model scenario #1) corresponding to each return period of water level, (a) 1 yr return period, (b) 2 yr return period, (c) 10 yr return period, (d) 20 yr return period.

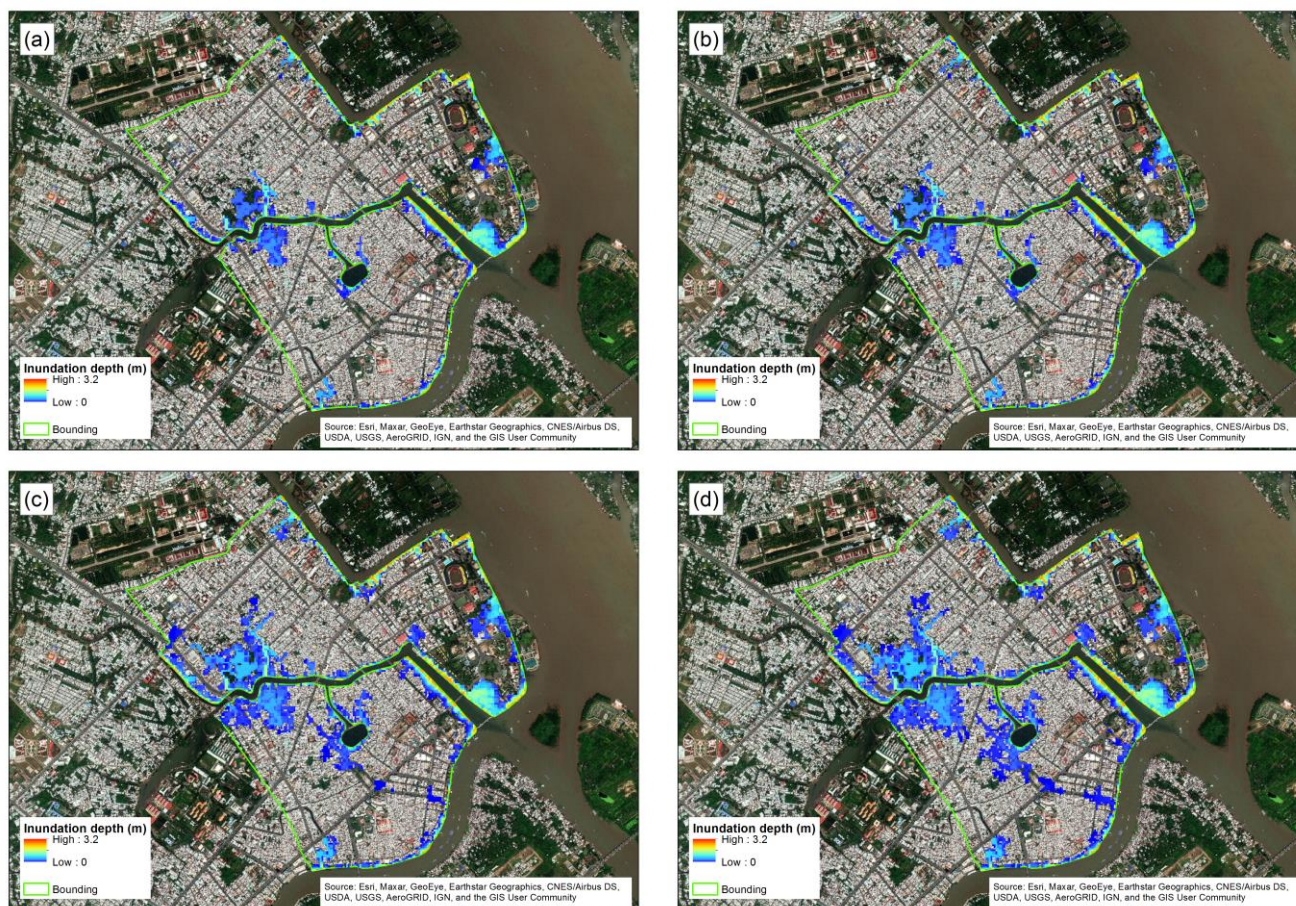


Figure A2: Flood hazard maps for 2050 under RCP 4.5 (model scenario #3) corresponding to each return period of water level, (a) 1 yr return period, (b) 2 yr return period, (c) 10 yr return period, (d) 20 yr return period.



Figure A3: Flood hazard maps for 2050 under RCP 8.5 (model scenario #5) corresponding to each return period of water level, (a) 1 yr return period, (b) 2 yr return period, (c) 10 yr return period, (d) 20 yr return period.

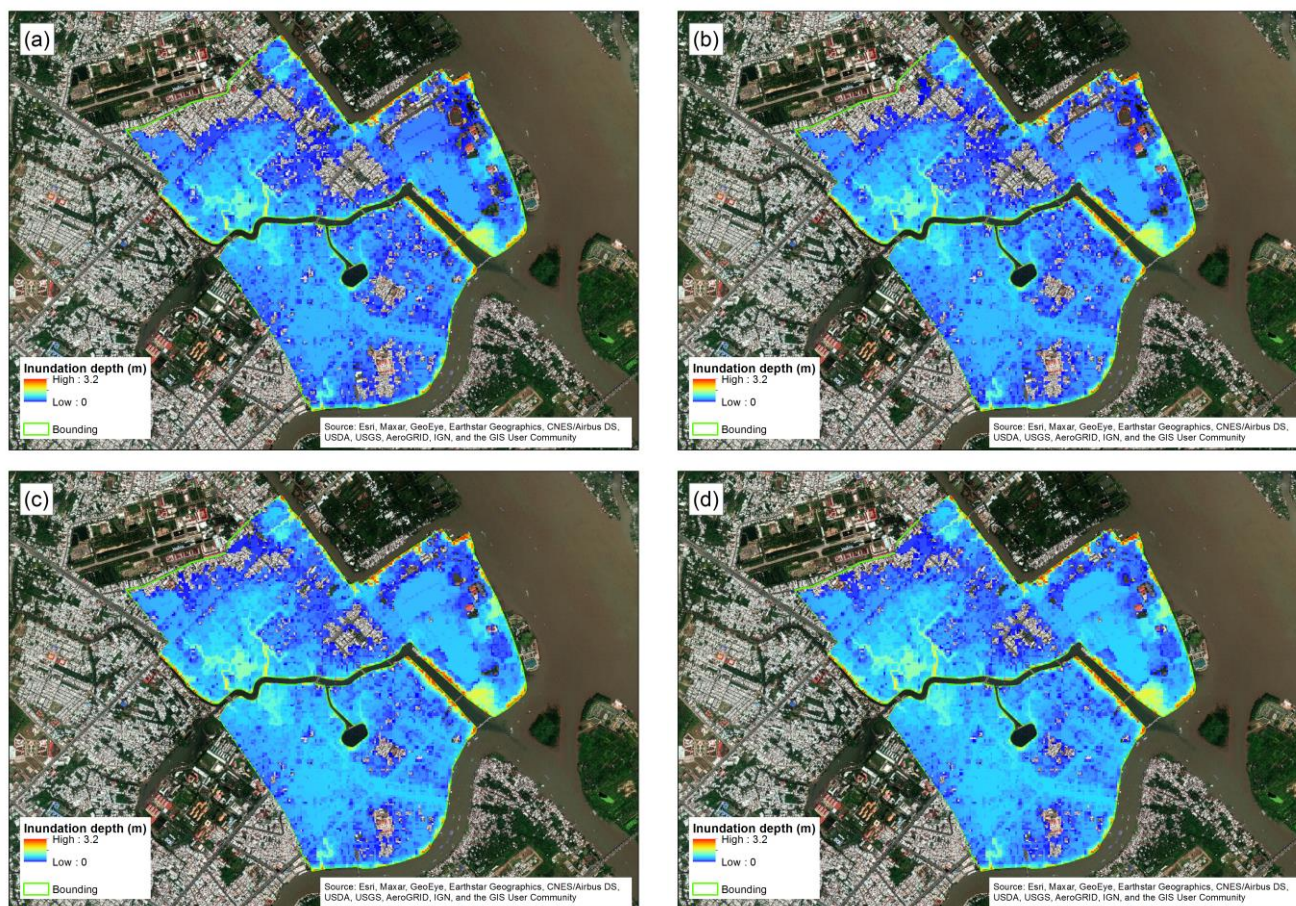


Figure A4: Flood hazard maps for 2050 under RCP 4.5 (model scenario #2) corresponding to each return period of water level, (a) 1 yr return period, (b) 2 yr return period, (c) 10 yr return period, (d) 20 yr return period.

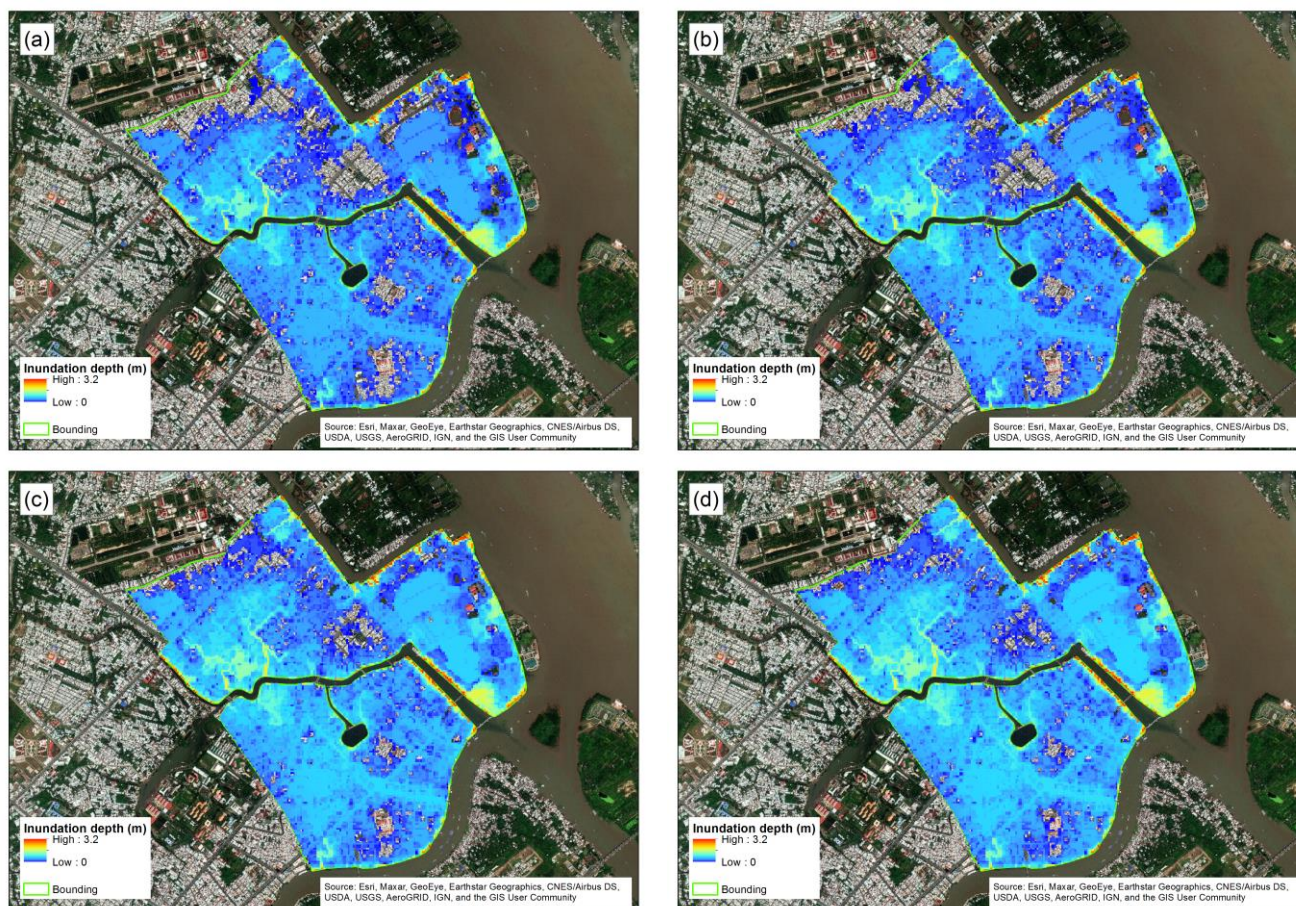


Figure A5: Flood hazard maps for 2050 under RCP 8.5 (model scenario #4) corresponding to each return period of water level, (a) 1 yr return period, (b) 2 yr return period, (c) 10 yr return period, (d) 20 yr return period.



Table 1. Data source used in this study

Data type	Source	Data description
Discharge	MRC	Daily discharge data at upstream from 2000 to 2006
Sea level (tide+surge)	GTSR data set (Muis et al., 2016)	Ten-minutely sea level data at the Mekong river mouths (Tran De, Ben Trai and An Thuan) from 1979 to 2014
Water level	National Hydro-Meteorological Service of Viet Nam	Hourly water level at Can Tho station on the 17 th of October 2016
Observed water depth	Measure	Minutely observed water depths in the manholes at Nguyen Van Cu and Tran Hung Dao streets on the 17 th of October 2016
DEM	Vietnam Institute of Meteorology, Hydrology and Environment	15 m resolution DEM for Ninh Kieu district

Table 2. Model scenarios adopted with the 1D/2D coupled flood PCSWMM model

Model scenario	Time	Climate scenario	Land subsidence rate
1	Present	-	-
2	2050	RCP 4.5	1.6 cm/yr
3	2050	RCP 4.5	0
4	2050	RCP 8.5	1.6 cm/yr
5	2050	RCP 8.5	0